Article

Initial Discovery and Characterization of Novel Spirotriazoloquinazolines as Potential Neuroprotectors: Synthesis, Computational Screening, and Preliminary In Vivo Evaluation

Kostiantyn Shabelnyk , Lyudmyla Antypenko [*] , Natalia Bohdan , Victor Ryzhenko , Igor Belenichev , Oleksandr Kamyshnyi , Serhii Kovalenko

Article

Initial Discovery and Characterization of Novel Spirotriazoloquinazolines as Potential Neuroprotectors: Synthesis, Computational Screening, and Preliminary *In Vivo* Evaluation

Kostiantyn Shabelnyk [1], Lyudmyla Antypenko [2]*, Natalia Bohdan [3], Victor Ryzhenko [1], Igor Belenichev [1], Oleksandr Kamyshnyi [2] and Serhii Kovalenko [5]

[1] Department of Pharmaceutical, Organic and Bioorganic Chemistry, Zaporizhzhia State Medical and Pharmaceutical University, 26 Maria Prymachenko Blvd., 69035, Zaporizhzhia, Ukraine

[2] Independent Researcher, 11 Lamana Str., 69063, Zaporizhzhia, Ukraine

[3] Institute of Organic Chemistry of the National Academy of Sciences of Ukraine, 5 Akademika Kukhara Str., 02094, Kyiv, Ukraine

[4] Department of Microbiology, Virology and Immunology, I. Horbachevsky Ternopil State Medical University, 46001 Ternopil, Ukraine

[5] Institute of Chemistry and Geology, Oles Honchar Dnipro National University, 72 Nauky Ave., 49010, Dnipro, Ukraine

*Correspondence: antypenkol@gmail.com

Abstract

Ketamine anesthesia frequently causes postoperative cognitive dysfunction as the primary clinical concern, with potential broader applications to trauma-related cognitive disorders. This study explores novel neuroprotectives, targeting multiple pathways through design, synthesis, and evaluation of forty 2'-R-6'*H*-spiro(cycloalkyl/heterocyclyl) [1,2,4]triazolo [1,5-*c*]quinazolines. Molecular docking showed superior binding affinities to GluA3 compared to references, additionally to favorable drug-likeness ADMET. Selected compounds were tested in ketamine-induced cognitive impairment rat models with assessment *in vivo*. Compounds **25**, **26**, and **32** effectively normalized ketamine-disrupted behavioral parameters, reducing anxiety and improving cognitive function more effectively than piracetam and fabomotizole. **31** showed potent anti-inflammatory effects (72% reduction in IL-1β, 80% - in caspase-1), while **26** enhanced cell survival pathways (96% increase in Bcl-2) and hypoxic adaptation (3.5-fold increase in HIF-1 mRNA). These novel spirotriazoloquinazolines function as positive modulators of cognitive-enhancing receptors (GABA(A), GluA3), rather than direct antagonists, demonstrating neuroprotective properties through anti-inflammatory, anti-apoptotic, and adaptive pathway modulation, while definitive classification requires functional validation.

Keywords: 2'-R-6'*H*-spiro(cycloalkyl-,heterocyclyl) [1,2,4]triazolo [1,5-*c*]quinazolines; neuroprotective activity; molecular docking; synthesis; ADMET; SAR

Introduction

Ketamine is a dissociative anesthetic widely used in medicine for the induction and maintenance of anesthesia. Ketamine anesthesia is applied in military field surgery because it enables simultaneous anesthesia for multiple patients and can save the lives of a significant number of casualties [1,2]. However, in military medicine, ketamine is not recommended for high-ranking officers due to concerns, that it may impair their professionalism and, consequently, lead to inadequate command decisions [3,4].

Currently, it is impossible to abandon ketamine due to its numerous positive properties. The drug remains the safest general anesthetic, unlike all other anesthesiologic agents, as it uniquely stimulates and supports the cardiovascular and respiratory systems [5]. Furthermore, many psychiatric side effects of ketamine can now be successfully managed, primarily through the use of neuroleptics (butyrophenone derivatives, benzodiazepines, and others), that correct unwanted changes [6,7].

However, the main problem with ketamine use is not related to intraoperative undesirable hemodynamic changes, but rather to long-term disturbances in the psycho-emotional sphere (sometimes lasting up to six months after ketamine anesthesia) [8]. Typically, such patients are not monitored by physicians after surgery, and subsequent deterioration of their cognitive functions and emotional state is rarely associated with ketamine's side effects.

Ketamine anesthesia can cause central nervous system (CNS) damage in the postoperative period, with postoperative cognitive dysfunction (POCD) being particularly significant. POCD can develop in patients of various age groups with no history of psychoneurological conditions. According to various authors [9–12], the frequency of POCD averages 36.8% of patients overall, ranges from 3% to 47% after cardiac surgery (with 42% of patients still affected 3-5 years after surgery), and from 7% to 26% after non-cardiac surgery (with 9.9% of patients affected for 3 months or more, and 1% of patients for over 2 years). Early POCD can lead to deterioration in patients' quality of life, specifically reducing their professionalism and level of socialization [13,14].

Among medications used to restore the psycho-emotional sphere in the postoperative period, piracetam is administered toward the end of surgery. However, there are extremely few other studies exploring pharmacological correction of POCD after ketamine. A neuroprotection concept has been proposed for POCD, aimed at timely restoration of neurochemical processes, cerebral hemodynamics, and elimination of cognitive-mnestic disorders [15]. The complexity of developing staged neuroprotection after POCD lies precisely in the lack of exact knowledge about the subtle mechanisms of ketamine's neurotoxic action.

Our earlier research established that ketamine, functioning as an NMDA receptor antagonist, paradoxically causes secondary excitotoxicity through activation of ROS production, neuroinflammation, and mitochondrial dysfunction. Our compounds are designed as neuroprotective modulators rather, than direct receptor antagonists, targeting the downstream pathological cascades rather than primary neurotransmitter blockade, and consequently, deterioration of spatial and working memory, increased anxiety, and more episodes of depressive behavior [16,17].

Currently, several nootropics have been proposed for POCD correction, including phenibut, ipacridine, cytoflavin, noopept, cerebrocurin, and thiocetam [18,19]. However, modern nootropic agents and neurometabolic neuroprotectors do not fully resolve the POCD problem. Racetams (piracetam, phenotropil, pramiracetam) enhance anxiety and positively modulate anaerobic glycolysis in neurons, which exacerbates lactate acidosis. Cerebrocurin provides rapid metabolic effects, activates energy metabolism, reduces neuroapoptosis and mitochondrial dysfunction, but does not affect amino-specific CNS systems such as GABA and serotonin, which play critical roles in the formation of anxiety, sadness, worry, anger, and emotional numbness [20–22].

All this necessitates the development and creation of entirely new structures that would have affinity for GABA and 5HT2A receptors, influence genes associated with the expression of specific amino-specific system intermediates and the function of the hypothalamic-pituitary-adrenal axis, as well as impact structural and functional abnormalities in the hippocampus, prefrontal cortex, amygdala, and other brain regions [23–25]. Currently, developing more effective medications with improved safety profiles to enhance cognitive function and treat anxiety disorders is an important task in medicinal chemistry. While our primary focus addresses POCD following ketamine anesthesia, the overlapping neurobiological mechanisms suggest potential broader therapeutic applications. POCD and trauma-related cognitive disorders share common pathways including

neuroinflammation, excitotoxicity, and disrupted neurotransmitter balance, justifying our multi-target approach.

The neurobiological mechanisms underlying POCD share significant overlap with stress-related cognitive disorders. The stress response system involves several key receptor interactions that are relevant to both ketamine-induced cognitive dysfunction and broader neuropsychiatric conditions. CRF1R mediates stress response and anxiety, GABA(A) receptors regulate anxiety and sleep disturbances, while serotonin receptors control mood and memory processing. This mechanistic convergence supports our multi-target therapeutic approach, with POCD as the primary indication and potential extension to stress-related cognitive disorders as secondary applications.

In terms of treatment potential, a multi-target approach might be more effective for complex conditions like POCD, with mechanistic insights potentially translatable to other stress-related cognitive disorders. Understanding receptor interactions could lead to more effective therapeutic strategies, with the potential for developing medications that address multiple symptoms simultaneously.

Based on the aforementioned considerations, our rational drug design strategy was directed toward combining the key structural features of various chemical classes of clinically confirmed pharmacophores (Figure 1, Table 1) and optimizing their molecules with saturated structural elements to increase lipophilicity and minimize toxicity.

Analysis of these reference compounds reveals essential pharmacophoric elements required for optimal nootropic and anxiolytic activity:

Core structure requirements

- Essential azoheterocyclic core
- *N*-methyl group for optimized GABA-A receptor binding
- Strategically positioned cycloalkyl/heterocyclyl rings for receptor pocket compatibility

Linking elements

- Azapirone structure with piperazine linker
- Specific alkylated terminal rings (pyrimidine, piperidine, pyridine, etc.)
- Optimal four-carbon spacing between cyclic systems

Stability and binding elements

- Cycloalkyl/alkyl groups for metabolic stability
- Multiple hydrogen bond donors/acceptors
- Flexible alkyl chains for conformational adaptation

Pharmacokinetic considerations

- Balanced lipophilicity for blood-brain barrier penetration
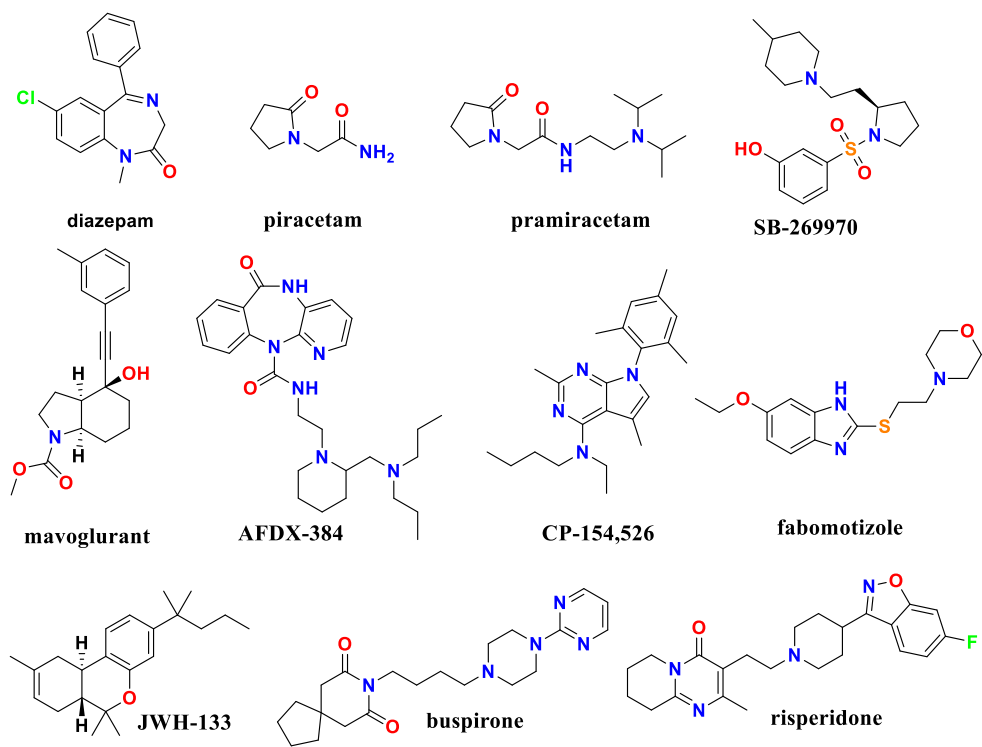
Figure 1. Nootropic and anxiolytic reference compounds chosen for rational drug design targeting POCD, with broader applicability to cognitive disorders sharing similar neurobiological pathways.

Table 1. Chemical classes of clinically confirmed pharmacophores selected for drug design according to the protein data bank targets.

| Compounds	Structural features	Mechanism of activity	Pharmacological effect
Diazepam	benzodiazepine	GABA-A receptor positive allosteric modulator ($\alpha1/\beta3/\gamma2L$)	sedative and muscle relaxant (anxiolytic) [26]
AFDX-384	benzodiazepine	muscarinic acetylcholine receptor antagonist (M_2 and M_4 subtypes)	treatment of dementia and schizophrenia [27]
Piracetam	pyrrolidine	AMPA receptor positive modulator and influences membrane fluidity, affecting ion transport and mitochondrial function	ootropic, used in cognitive impairment and myoclonus [28]
Pramiracetam	pyrrolidine	glutamate receptor 3 (GluA3)	nootropic stimulant [29]
SB-269970	pyrrolidine	selective 5-HT_7 receptor antagonist	treatment of anxiety and depression and nootropic effects [30]
Mavoglurant	indole	antagonist of the metabotropic glutamate receptor 5 (mGluR5)	obsessive-compulsive disorder [31]

Fabomotizole	benzimidazole	selective MT3 (sigma-1) receptor ligand with anxiolytic properties	anxiolytic and neuroprotective agent [32]
CP-154,526	pyrrolo [3,2-*e*]-pyrimidine	corticotropin-releasing factor receptor 1 (CRF1R)	treatment of alcoholism [33]
JWH-133	tetrahydrobenzo [*c*]–chromene	cannabinoid (CB$_2$) receptor agonist, G protein coupled receptor	anxiolytic [34]
Buspirone	azaspiro [4.5]decane	serotonin 5-HT$_{1A}$ receptor partial agonist	anxiolytic (treat anxiety disorders) [35]
Risperidone	1,2-benzoxazol; pyrido [1,2-*a*]–pyrimidine	5-HT (5-HT$_{2C}$, 5-HT$_{2A}$) receptors antagonist, D2 dopamine receptor	antipsychotic, anxiolytic [36]

Note: GABA-A: gamma-aminobutyric acid type A receptor; AMPA: α-amino-3-hydroxy-5-methyl-4-isoxazole propionic acid receptor; 5-HT: 5-hydroxytryptamine (serotonin) receptor; mGluR5: metabotropic glutamate receptor 5; CRF1R: corticotropin-releasing factor receptor 1; CB$_2$: cannabinoid receptor type 2. Target selection was guided by relevance to cognitive enhancement, anxiety modulation, and neuroprotection. Structural features were analyzed to identify key pharmacophoric elements essential for receptor binding and biological activity.

The foundation of our rational design for promising bioactive substances is based on the modern experience of merging molecular fragments through spiro-conjunction. Moreover, azaheterocycles fused with spirocyclic fragments represent an exceptional tool in drug development, allowing for the adjustment of conformational and physicochemical properties of the investigated molecule [37–39].

The main advantage characteristic of this class of compounds is their inherent three-dimensional nature, which is beneficial for ligand interactions with the three-dimensional binding site of a biotarget. Another advantage is their solubility, which is associated with the high content of sp³-hybridized Carbon atoms. Importantly, this advantage liberates "lead compounds" from many pharmaco-technological and pharmacokinetic obligations that arise when implementing typical aromatic or heterocyclic structures. Furthermore, spiroheterocycles exhibit a broad spectrum of biological activities, including anti-inflammatory, anticonvulsant, antiproliferative, antimalarial, antimicrobial, and other types of activity [37–42]. Therefore, the fusion of two molecular fragments was decided to be conducted *via* a 5+1-heterocyclization reaction involving triazoloanilines and cycloalkanones (Figure 2).
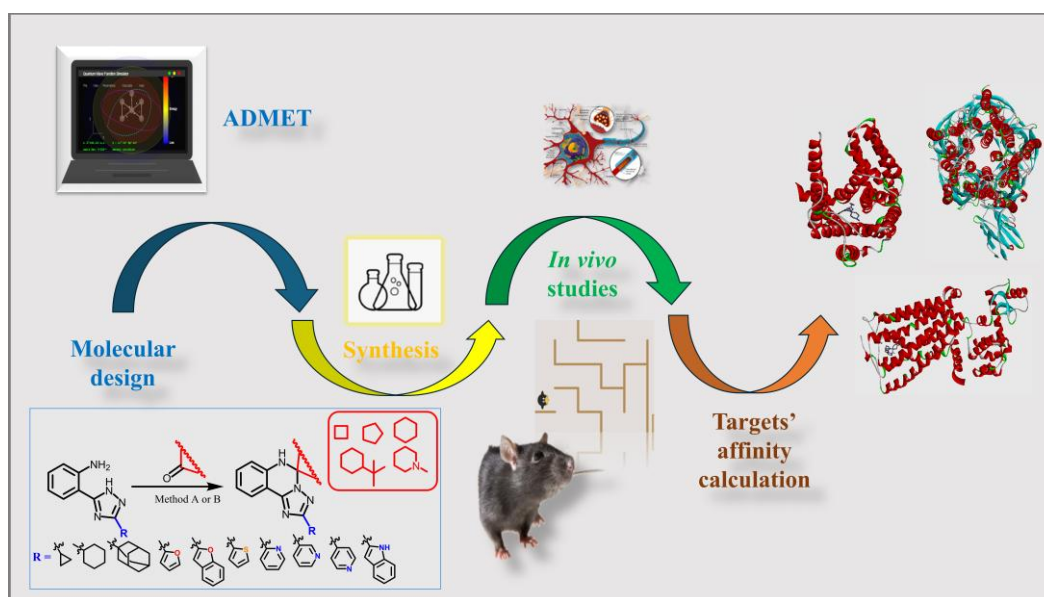
Figure 2. Design and research methodology among 2′-R-6'*H*-spiro(cycloalkyl-,heterocyclyl)– [1,2,4]triazolo [1,5-*c*]quinazolines.

Hence, to address above-mentioned challenges in treating cognitive and behavioral disorders following ketamine anesthesia, we employed a comprehensive research strategy combining computational design, organic synthesis, and biological evaluation. Our approach focused on developing novel spiro(cycloalkyl-,heterocyclyl) [1,2,4]triazolo [1,5-*c*]quinazolines with improved target engagement profiles and reduced side effects compared to existing agents. The comprehensive methodological approach enabled systematic investigation of novel compounds from molecular design through behavioral and neurobiochemical evaluation. In the following sections, we present the results of these studies, beginning with *in silico* computational analyses and progressing to *in vivo* efficacy and mechanism evaluations.

Results and Discussion

In Silico Preliminary Check of Nootropic Potential

The main target for assessing the nootropic potential of the developed compounds was chosen glutamate receptor GluA3 (RCSB ID: 3LSX), due to its established role in the mechanisms of improving cognitive functions [43]. This ionotropic receptor mediates rapid excitatory synaptic transmission in the central nervous system and plays crucial roles in synaptic plasticity, learning, and memory processes. The selection of GluA3 as a target is particularly relevant given its involvement in cognitive enhancement pathways and its well-characterized structural interactions with established nootropics like piracetam [29,43]. Additionally, this receptor's role in neuroplasticity and potential therapeutic applications makes it an attractive target for novel cognitive enhancers [44].

The binding interactions were analyzed using the CB-Dock2 methodology for protein-ligand blind docking, incorporating cavity detection and homologous template fitting as described by Liu *et al.* [45] (Figure 3, Supplementary Materials, Table S1).
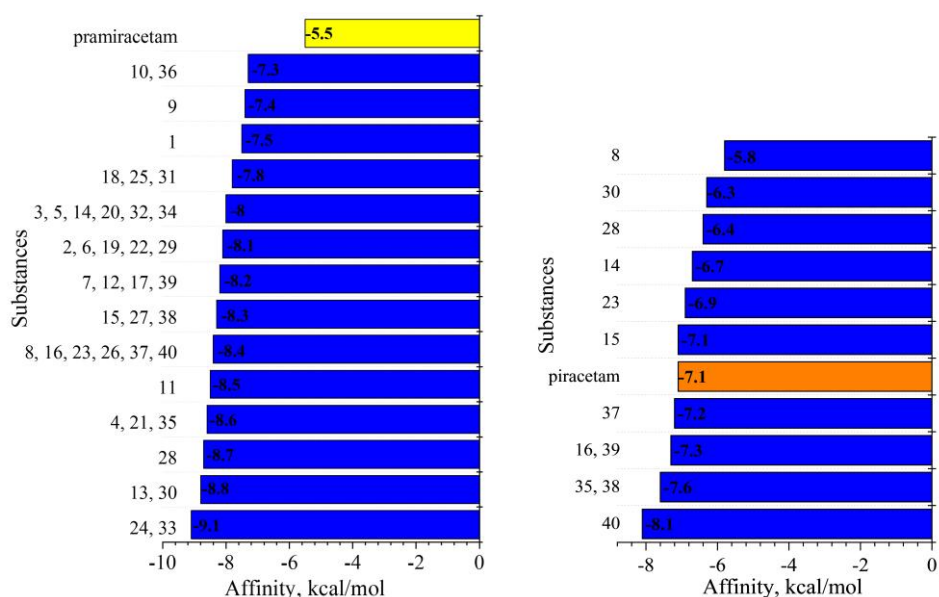
Figure 3. Comparative binding affinities of designed compounds to glutamate receptor 3 (GluA3) crystal structure (RCSB PDB ID: 3LSX). Left panel: Pramiracetam binding pocket (cavity volume: 126 Å³; center coordinates: −5, 22, 19; docking dimensions: 17 × 17 × 17 Å). Right panel: Piracetam binding pocket (cavity volume: 507 Å³; center coordinates: −12, 14, 21; docking dimensions: 19 × 19 × 19 Å).

Molecular docking analysis revealed, that 13 compounds of 40 demonstrated binding affinities exceeding −7.3 kcal/mol within the GluA3 active pocket, surpassing the reference compound piracetam serving as a reference compound, that exhibited relatively weak binding affinity (−5.5 kcal/mol). This observation aligns with established structural studies of α-amino-3-hydroxy-5-methyl-4-isoxazolepropionic acid (AMPA) receptor interactions, particularly the work of Ahmed and Oswald [43], who demonstrated that related racetam compounds interact through distinct allosteric binding sites. AMPA receptors are tetramers composed of combinations of four subunits (GluA1-GluA4), which can assemble in various combinations to form functional channels.

The found modest binding affinity is consistent with recent systematic reviews of racetam efficacy by Gouhie *et al.* [29], which found variable cognitive enhancement outcomes in clinical settings, suggesting that direct GluA3 interaction may not be the primary mechanism of action. This mechanistic complexity is further supported by recent analyses of nootropic compounds that highlight the diverse molecular pathways involved in cognitive enhancement [46]. Moreover, the comprehensive review by Jędrejko [46] and colleagues also revealed that nootropic compounds can act through multiple mechanisms, including modulation of neurotransmitter systems, enhancement of neuronal metabolism, improvement of cerebral blood flow, and influence on neuroplasticity pathways.

So, the majority of synthesized compounds demonstrated binding affinities exceeding −8.0 kcal/mol against the target receptor, suggesting significant nootropic potential. Among which compounds **24** and **33** (−9.1 kcal/mol) show the strongest binding. Compound **24** is 2'-(pyridin-3-yl)-6'*H*-spiro [cyclohexane-1,5'- [1,2,4]triazolo [1,5-*c*]quinazoline], while **33** is 2'-(adamantan-1-yl)-1-methyl-6'*H*-spiro [piperidine-4,5'- [1,2,4]triazolo [1,5-*c*]quinazoline]. Compounds **13**, **30**, **28**, **4**, **21**, **35** features preferably heterocyclic rings like benzofuran, furan, and thiophene, and show high-medium affinity (−8.8 to −8.5 kcal/mol). Medium affinity (−8.4 to −8.0 kcal/mol) is shown by group of compounds including **11**, **8**, **16**, **23**, **26**, **37**, and **40**, etc. bearing various substituents at R position. Lower affinity (below −8.0 kcal/mol) notably includes compounds **1**, **9**, **10**, and **36** with smaller ring systems.

Moreover, the recent analysis of spiro [1,5'/4,5'- [1,2,4]triazolo [1,5-*c*]quinazoline] derivatives and their interaction with $\alpha 1/\beta 3/\gamma 2L$ GABA(A) receptors (RCSB PDB ID: 6HUP) revealed important structure-activity relationships (Table S2) [47]. Our findings indicate that an optimal balance between

structural rigidity and conformational flexibility appears essential for maintaining effective binding interactions. Compounds containing expanded ring systems exhibited enhanced binding affinity, with calculated binding energies ranging from −12.4 to −11.8 kcal/mol. The strategic positioning of hydrogen bond donors and acceptors within these molecular structures contributed significantly to specific receptor interactions. Interestingly, the incorporation of electron-rich heterocyclic systems, particularly furan and thiophene moieties, generally resulted in diminished binding affinity, likely due to unfavorable electronic distribution patterns that disrupted optimal ligand-receptor interactions.

While molecular docking analyses provide binding affinity predictions, these computational results cannot definitively distinguish between agonist, antagonist, or allosteric modulator activity. The observed binding energies indicate target engagement potential but require experimental validation to determine functional outcomes. Current evidence suggests positive modulation based on behavioral profiles, but direct receptor activation studies remain necessary for definitive pharmacological classification. Nevertheless, the promising molecular docking results provided a strong rationale for proceeding with the synthesis of these compounds. Our synthetic efforts successfully delivered the target molecules in good to excellent yields, enabling further characterization and biological evaluation. However, *in vivo* experimental validation would be crucial to confirm cognitive enhancement effects, evaluate side effect profiles, determine optimal dosing and administration, and assess long-term safety and efficacy.

Synthesis

One of the approaches for constructing spiro derivatives is the [5+1]-cyclocondensation reactions, based on the interaction of 1,5-binucleophiles with carbonyl compounds [41]. Similarly, spiro [1,2,4]triazoloquinazolines (**1**-**40**) were obtained, specifically through the interaction of [2-(3-R-1*H*-1,2,4-triazol-5-yl)phenyl]amines (**a**) with cycloalkanones (cyclobutanone, cyclopentanone, cyclohexanone, 4-*tert*-butylcyclohexanone) or *N*-methylpiperidone (Figure 4).

The cyclocondensation proceeded without peculiarities in propan-2-ol in the presence of a catalytic amount of sulfuric acid, following a mechanism that included three main processes: carbinolamine formation, elimination of a water molecule, and intramolecular cyclization [48]. The target products are formed with satisfactory and high yields (67-95%) (Supplementary Materials, Spectral data). Furthermore, the reaction also proceeds in other organic solvents that are miscible with water and indifferent to the starting amines.

The formation of compounds **1**-**40** was confirmed by chromatography-mass spectrometry, ^{1}H and ^{13}C NMR spectra, and elemental analysis. In the ^{1}H NMR spectra, the aromatic protons of the heterocycle form a characteristic ABCD system, which is represented by two doublets (H-7, H-9) and two triplets (H-8, H-10) with corresponding chemical shifts [41]. The characteristic proton of the NH-group (position 6) for these compounds is observed in the spectrum as a singlet in a wide range (7.22-3.79 ppm), and its chemical shift is determined by the donor-acceptor properties of the substituents in positions **2** and **5**. In some compounds, the signal of this proton is absent or resonates together with the aromatic protons of the quinazoline cycle. The proton signals of the spiro-condensed fragment in position 6' and the substituent in position 2 of compounds **1**-**40** in most cases are easily interpreted and have classical shifts and multiplicity [49]. The ^{13}C NMR spectra of compounds additionally confirm the regioselective course of the [5+1]cyclocondensation reaction. Thus, the characteristic signals of the sp^3-hybridized Carbon atom in position 1,5' were observed at 83.1-70.0 ppm.
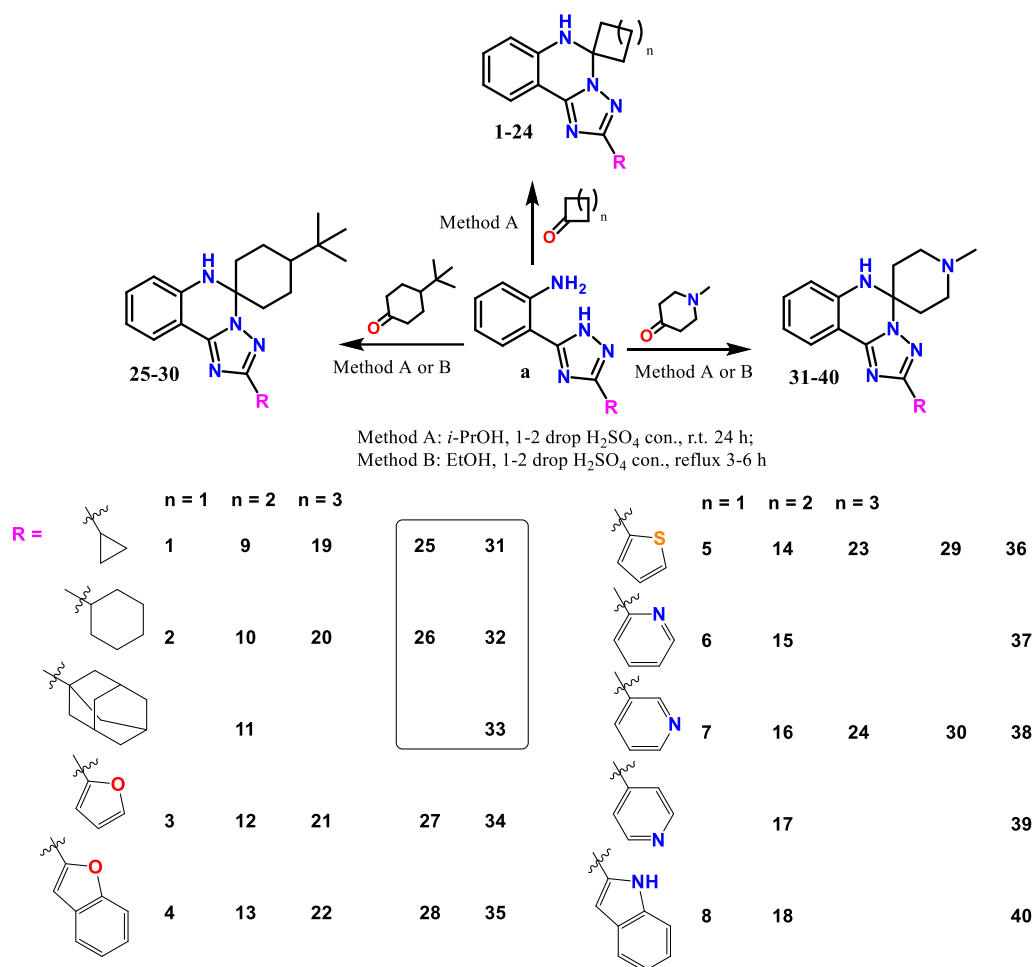
Figure 4. Synthetic route to 2'-R-6'*H*-spiro(cycloalkyl-,heterocyclyl) [1,2,4]triazolo [1,5-*c*]quinazolines (**1-40**) *via* acid-catalyzed condensation. Substances in the frame are chosen for *in vivo* studies.

Following successful synthesis and structural confirmation of compounds **1**-**40**, we proceeded to evaluate their safety profiles through comprehensive toxicity prediction studies. This critical step in our investigation aimed to identify compounds with optimal therapeutic indices for subsequent biological evaluation.

In silico ADMET Studies

For *in vivo* study, we selected 5 compounds: **25**, **26**, **31**-**33**. The selection represents distinct structural variations (different R-groups or spiro-cyclic/heterocyclic systems) to explore structure-activity relationship of activity: spiro-junction of cyclohexane *vs.* *N*-methylpiperidine; 2'-position substituent: cyclopropyl *vs.* cyclohexyl *vs.* adamantyl; additional substituents: *tert*-butyl group in compounds **25** and **26**. Besides these compounds show consistently low toxicity predictions across multiple parameters [50] compared to other compounds in the series (Table 2). ProTox-II [51] and SwissADME analysis [52] were conducted to determine their compliance with toxicity and drug-likeness criteria. The results of the toxicity study showed that these compounds, like piracetam and fabomotizole that were chosen as references for further *in vivo* studies, belong to toxicity class IV. All compounds are distinctive for showing "no" predictions for all toxicity parameters evaluated, indicating a potentially safer pharmacological profile. Still, cytotoxicity is predicted for all mentioned substances, except **25** and **26**.

Table 2. Predicted toxicity of the compounds selected for the study *in vivo*.

Sub.	Toxicity index	LD$_{50}$, mg/kg	Pred. acc., %	HT	CG	IT	MG	CT
25	IV	2000	54.26	0.63	0.50	0.92	0.59	0.53
26		2000		0.65	0.50	0.95	0.61	0.53
31		1200		0.73	0.50	0.96	0.57	0.60/yes
32		2000		0.76	0.53	0.97	0.61	0.60/yes
33		1200		0.76	0.53	0.99	0.61	0.60/yes
fabomotizole		677		0.62	0.53	0.85	0.65	0.59/yes
piracetam		2000	100	0.95	0.61	0.99	0.84	0.62/yes

Note: Class IV: harmful if swallowed ($300 < \text{LD}_{50} \leq 2000$). Pred. acc.: prediction accuracy. Toxicity parameters measured on a 0-1 scale with higher values indicating greater potential toxicity: HT: Hepatotoxicity; CG: Carcinogenicity; IT: Immunotoxicity; MG: Mutagenicity; CT: Cytotoxicity (yes indicate potential cytotoxic effect).

While toxicity assessment provided valuable safety data, understanding the pharmacokinetic behavior of these compounds was equally important for their potential development as therapeutic agents. Therefore, we next examined their drug-likeness parameters and predicted ADME profiles to identify candidates with optimal bioavailability and blood-brain barrier penetration (Table 3) [50].

Hence, most of the studied compounds, like the reference drugs, meet the criteria for drug-likeness: MW (Da) (< 500), n-HBA (< 10), n-HBD (≤ 5), TPSA (< 140 Å²) and logP (≤ 5). The satisfactory TPSA value (> 140 Å²) for all compounds also correlates well with passive molecular transport across membranes. That is, the studied compounds will have a high ability to penetrate the blood-brain barrier and flexibly interact with molecular targets. Additionally, the studied compounds show high predicted bioavailability. An exception to these criteria is compound **26**, which has a high lipophilicity value (logP = 5.14), which can also be a positive characteristic, taking into account the structure of the neuron membrane. Importantly, the studied compounds pass the "drug-likeness" criteria for all filters (Lipinski, Veber, Muegge, Ghose, Egan), which are widely used in drug design. Only compound **25** and **26** piracetam have few violations of Veber and Egan filters.

Moreover, all compounds in this study were evaluated against Brenk structural filters and Pan-Assay Interference compounds (PAINS) criteria. No structural alerts were identified, suggesting a reduced likelihood of false positives or reactive functionalities in the tested chemical series. However, absence of these alerts does not guarantee lack of other potential mechanisms of interference, and standard validation protocols were still employed.

In comparison to reference drugs included in the analysis (piracetam and fabomotizole), the novel spiro [1,2,4]triazolo [1,5-*c*]quinazoline derivatives exhibited generally higher molecular weights and aromaticity, but comparable or lower rotatable bond counts and polar surface areas.

Notably, fabomotizole contained significantly more rotatable bonds (6) than any of the novel compounds (1-2), suggesting the designed derivatives may benefit from reduced conformational entropy penalties upon binding. Piracetam, a marketed nootropic drug included as a reference, failed to meet several Ghose criteria due to its small size (MW < 160) and low lipophilicity (WLOGP < −0.4). This observation suggests that compounds with minor violations may still represent *via*ble drug candidates, particularly when strong target engagement is demonstrated. As well as marketed drugs do not always conform to all druggability filters, particularly those with unique physicochemical properties or specific mechanisms of action.

Table 3. Physicochemical descriptors and pharmacokinetic properties of chosen compounds provided by SwissADME.

Descriptors	Compounds

and properties	25	26	31	32	33	piracetam	fabomotizole
MW (Da)	336.47	378.55	295.38	337.46	389.54	142.16	307.41
n-ROTB	2	2	1	1	1	2	6
n-HBA	2	2	3	3	3	4	4
n-HBD	1	1	1	1	1	6	1
TPSA	42.74	42.74	45.98	45.98	45.98	63.40	75.68
Consensus	4.21	5.14	2.20	3.16	3.71	−0.64	2.30
Molar refractivity	105.28	119.70	93.12	107.54	122.42	38.76	88.93
Gastrointestinal absorption	high						
Blood–brain barrier permeation	yes					no	yes
Drug likeness							
Lipinski (Pfizer); Muegge (Bayer); Ghose rules	yes						
Veber (GSK) rules	yes					no/MW<160, WLOGP <−0.4, MR<40	yes
Egan filter	no/XLOGP3>5	yes				no/MW<200	yes
Lead-likeness	no	yes				no	yes
Bioavailability Score	0.55						
Brenk alert, PAINS	no alerts						

Note: MW: Molecular weight; n-ROTB: number of rotatable bonds; n-HBA: number of Hydrogen bond acceptors; n-HBD: number of Hydrogen bond donors; TPSA: topological polar surface area; logP: octanol-water partition coefficient. "Yes" indicates the compound meets all criteria for the specified rule; "no" followed by specific parameters indicates which criteria were not met. Lipinski's Rule of Five states that an orally active drug generally has no more than one violation of the following criteria: MW ≤ 500 Da, logP ≤ 5, n-HBD ≤ 5, and n-HBA ≤ 10. Compounds violating more than one of these parameters are predicted to have poor absorption or permeation. Muegge (Bayer) rules evaluate drug-likeness based on the following parameters: MW: 200-600 Da; logP: -2 to 5; TPSA: ≤ 150 Å²; n-ROTB: ≤ 15; n-HBD: ≤ 5; n-HBA: ≤ 10; number of rings: ≤ 7; number of carbons: > 4; number of heteroatoms: > 1. Ghose rules define drug-like molecules as those with: MW: 160-480 Da; logP: -0.4 to 5.6; molar refractivity: 40-130; total number of atoms: 20-70; n-HBD: ≤ 5; n-HBA: ≤ 10. Egan filter evaluates compounds based on TPSA and WLOGP to predict passive intestinal absorption. Compounds with TPSA > 131.6 Å² and WLOGP > 5.88 are predicted to have poor absorption. Veber (GSK) rules: compounds are considered drug-like when they have ≤ 10 rotatable bonds and TPSA ≤ 140 Å². Brenk filter identifies structural fragments that may cause undesired reactivity, toxicity, or poor metabolic properties. PAINS (Pan-Assay Interference Compounds) filter identifies substructures that frequently cause false positives in high-throughput screening assays. "No alerts" alerts indicates compounds passed all criteria for the specified filter. The bioavailability score represents the probability of a compound having at least 10% oral bioavailability in rats or measurable Caco-2 permeability.

Also, interestingly, that reference compounds demonstrated markedly different solubility profiles. Piracetam exhibited exceptional water solubility across all three models (classified as "highly soluble" by ESOL and Ali), consistent with its low molecular weight and hydrophilic character.

Fabomotizole showed moderate solubility comparable to many of the novel derivatives, supporting the potential pharmaceutical *via*bility of compounds with similar solubility profiles. Latter also demonstrated BBB penetration. And piracetam, as expected from its highly hydrophilic nature, showed no BBB penetration, consistent with its well-established favorable safety profile, but limited brain exposure.

Based on the favorable safety and pharmacokinetic profiles identified through *in silico* analyses, selected five representative compounds (**25**, **26**, **31-33**) were approved for in-depth biological evaluation. A systematic three-tier selection process was employed:

Tier 1 - Computational screening (40 compounds → 13 candidates)

- GluA3 binding affinity > −7.3 kcal/mol (exceeding piracetam reference)

- Favorable ADMET predictions (toxicity class IV, drug-likeness compliance)

Tier 2 - Structure diversity analysis (13 candidates → 5 compounds)

- Representative spiro-junction types: cyclohexane (**25**, **26**) *vs. N*-methylpiperidine (**31**, **32**, **33**)

- Diverse 2'-substituents: cyclopropyl (**25**, **31**), cyclohexyl (**26**, **32**), adamantyl (**33**)

- Additional structural features: *tert*-butyl substitution (**25**, **26**)

Tier 3 - Risk-benefit assessment (5 compounds selected, **25**, **26**, **31-33**)

- Lowest predicted cytotoxicity: compounds **25**, **26** (no cytotoxic alerts)

- Balanced multi-target engagement profiles

- Optimal blood-brain barrier penetration predictions

These compounds were chosen to represent key low toxic structural variations within our library, allowing for meaningful structure-activity relationship determinations in physiologically relevant models.

In Vivo Activity

Open Field Test Following Ketamine Anesthesia

The ketamine-induced cognitive impairment paradigm was selected as the primary screening model for evaluating novel nootropic compounds [53–55]. This model demonstrates particular relevance for our structure-based approach due to the overlapping mechanisms between our target compounds and ketamine in glutamatergic and monoaminergic systems.

Our study primarily targets POCD following ketamine anesthesia. The ketamine-induced cognitive impairment model serves as our primary validation system, with mechanistic insights potentially applicable to broader cognitive disorders sharing similar neurobiological pathways. The ketamine model offers several advantages for evaluating novel compounds.

First, ketamine's well-characterized antagonism of NMDA receptors produces reproducible cognitive deficits that can be quantitatively measured. Second, these deficits share neurochemical similarities with a variety of clinical conditions where cognitive improvement is desired. Third, the model allows us to assess both direct cognitive enhancement and the ability to reverse the induced deficit, providing additional insights into the mechanisms of action of our compounds. Furthermore, this model is particularly relevant for the evaluation of compounds structurally related to reference molecules in our study, as these agents often act through glutamate-dependent mechanisms. Thus, the ketamine model provides a mechanistically relevant framework for evaluating our structural approach to drug development.

So, analysis of specific behavioral indicators in the open field test revealed that ketamine anesthesia significantly altered the behavioral characteristics of experimental animals (Table S3, Figure 5).

Administration of ketamine (control group) led to a significant increase in total motor activity (48862.22±3612.2 cm²/s *vs.* 24175.01±2839.76 cm²/s in intact animals) and distance traveled by animals two days post-anesthesia (Table S3, Figure 5). Notably, free distance increased both in absolute units (604.8±32.71 cm *vs.* 59.37±26.31 cm in intact animals) and as a percentage of total motor activity (11.43±1% *vs.* 1.43±0.61%), representing an approximately 10-fold increase. Significant aggression was observed in animals two days after anesthesia. Additionally, the control group exhibited a 1.86-fold

increase in freezing episodes (529±27 *vs.* 284±35 units) and a 1.5-fold increase in immobility (429±27 *vs.* 284±35 units). These behavioral changes collectively indicate the development of anxiety and heightened excitability in animals following ketamine anesthesia.

Ketamine administration did not affect the number of free rearings, but significantly increased rearings near the wall by 2.25-fold (9±1 *vs.* 4±1 units). Furthermore, the frequency of short grooming acts decreased by 4-fold (1±1 *vs.* 4±1 units) while extended grooming remained unchanged. These observations further support increased anxiety, excitability, and diminished comfort in ketamine-treated animals. The control group also demonstrated a 2-fold increase in high activity duration (15.12±1.63% *vs.* 7.83±1.87%), indicating elevated emotionality and excitability. This increased high activity can be interpreted as reduced efficiency in exploratory and search behaviors, as animals perform excessive "unnecessary" movements and require more time to adapt to novel environments.
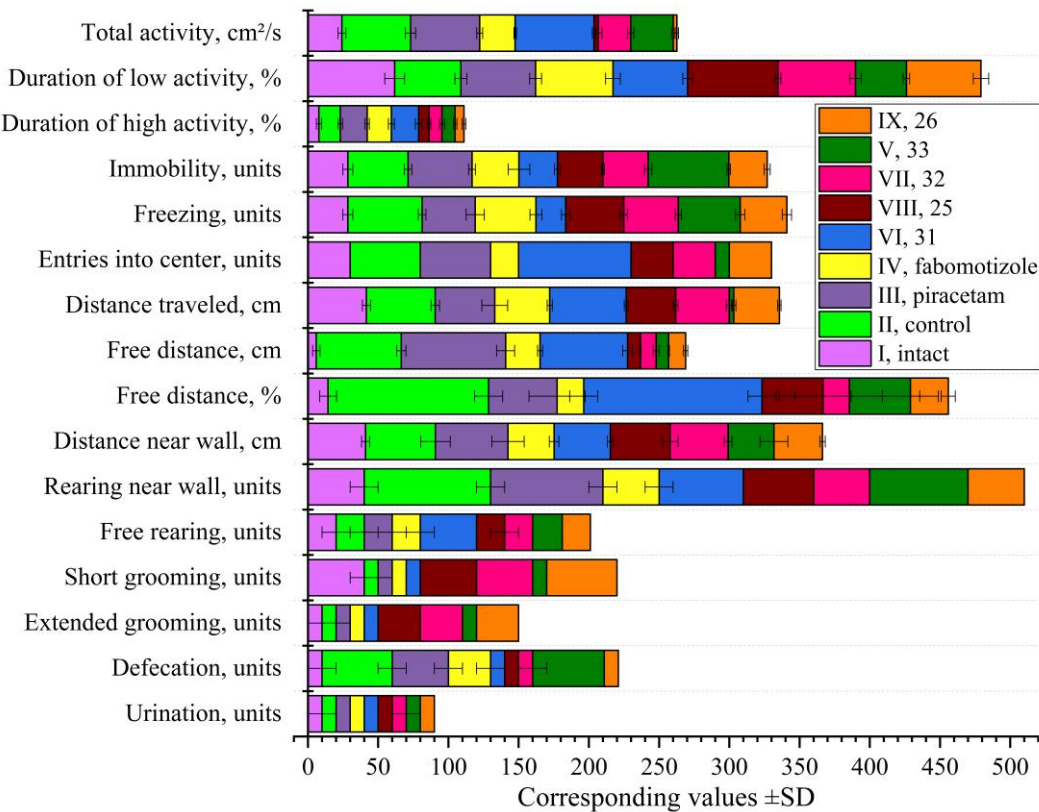
Figure 5. Comparative behavioral profile of experimental compounds on locomotor activity, exploratory behavior, and anxiety-like responses in the Open Field test following ketamine anesthesia. Data presented as normalized values (±SD) in ascending order of their sum for each studied compound from **26** to **31**. Data normalized for scale compatibility: total activity (cm²/s) divided by 1000; distance traveled and near wall distance (cm) divided by 100; immobility, freezing (units), and free distance (cm) divided by 10; free distance (%), number of entries into center, rearing near wall, free rearing, short grooming, extended grooming, defecation, urination (units) multiplied by 10. Significant differences ($p<0.05$) are found between treatment groups and either intact or control animals.

Regarding the reference compounds, piracetam administration increased free distance compared to both intact and control groups (743.3±64.21 cm), but failed to reduce freezing episodes (378±65 units) or immobility (455±24 units), both remaining significantly higher than intact values. The number of wall rearings under piracetam remained elevated compared to the intact group (8±1 *vs.* 4±1 units), while short grooming acts remained at the control level (lower than intact values), and defecation frequency remained elevated (4±1 *vs.* 1±1 units in intact animals). These observations suggest that piracetam not only failed to reduce anxiety and fear following ketamine anesthesia but potentially exacerbated these states and the associated discomfort.

In contrast, fabomotizole significantly reduced free distance compared to control (245.32±18.23 cm *vs.* 604.8±32.71 cm), normalized immobility (334±77 units), and modestly reduced freezing episodes (432±42 *vs.* 529±27 units), though the latter remained significantly higher than intact values. However, fabomotizole did not normalize wall rearings, had minimal effects on high and low activity durations, and did not affect grooming behavior. These data indicate that fabomotizole partially reduces anxiety and fear after ketamine anesthesia but has limited impact on animal discomfort and cognitive activity.

Administration of tested compound in 10 mg/kg, namely **33** led to significant reductions in overall activity compared to the control group, though still elevated above intact levels (30321.33±1244.3 cm²/s). This group exhibited a pronounced alteration in activity structure, with a significant increase in immobility episodes (574±121 units). Compound **33** did not significantly reduce distance traveled but did decrease both high activity (9.33±1.22% *vs.* 15.12±1.63% in control) and low activity (36.21±2.33% *vs.* 47.11±4.22% in control and 61.71±7.08% in intact) durations. Animals displayed low mobility and preference for dark corners during testing, suggesting suppression of exploratory and cognitive activities. The number of center entries decreased (1 *vs.* 5 in control), potentially indicating either suppressed cognitive activity or persistent anxiety, despite reduced freezing episodes compared to control.

Compound **31** effectively reduced aggression following ketamine anesthesia while promoting active exploratory behavior. Animals receiving this compound showed significantly increased total activity compared to both control and intact groups (56177.4±1276.8 cm²/s). High activity duration was significantly increased (19.4±2.33%), suggesting enhanced cognitive engagement. The increased number of center entries (8 *vs.* 5 in control) and free rearings (4±1 *vs.* 2±1 units) further support improved exploratory behavior. However, the elevated free distance (622.3±34.3 cm), particularly in the context of increased high activity, may indicate somewhat inefficient exploratory patterns with excessive movements. Importantly, compound **31** significantly reduced anxiety markers, as evidenced by decreased freezing episodes (212±31 *vs.* 529±27 units), reduced immobility (274±21 *vs.* 429±27 units), increased center entries, and reduced defecation (1±1 *vs.* 5±1 units). These findings suggest a potential disinhibitory effect of compound **31.**

Compounds **25**, **26**, and **32** demonstrated particularly favorable behavioral profiles. All three compounds effectively reduced post-ketamine aggression while normalizing total activity to near-intact levels. Each compound significantly normalized high activity duration compared to control, while compound **25** additionally increased low activity duration (64.22±2.12% *vs.* 47.11±4.22% in control), suggesting enhanced quality of exploratory and cognitive behaviors. All three compounds significantly reduced freezing episodes and immobility, indicating anxiolytic effects.

Notably, compounds **25**, **26**, and **32** significantly reduced free distance, suggesting improved efficiency of exploratory activity. The number of center entries normalized to intact levels (3 entries), further supporting normalized cognitive function. Animals receiving these compounds also exhibited significantly increased short (4±1, 4±1, and 5±1 units, respectively, *vs.* 1±1 in control) and extended grooming (3±1 units for all three *vs.* 1±1 in control), along with decreased defecation (1±1 units for all three *vs.* 5±1 in control), indicating reduced anxiety and aggression alongside increased comfort.

In summary, the behavioral analysis in the open field test following ketamine anesthesia revealed that compounds **25**, **26**, and **32** exhibited the most favorable profiles among all tested substances. These compounds effectively normalized behavioral parameters disrupted by ketamine through positive modulation rather than inhibition of key systems. The anxiolytic effects suggest GABA(A) positive allosteric modulation (enhancement without sedation), while cognitive improvements indicate glutamate receptor positive modulation (facilitation rather than blockade). However, these behavioral inferences require confirmation through direct functional assays, as similar behavioral outcomes could theoretically result from different receptor interaction mechanisms depending on circuit-level effects and compensatory pathways.

Compound **31** demonstrated potent anxiolytic and stimulatory effects but may promote somewhat inefficient exploratory behavior. Compound **33** showed mixed effects with some anxiolytic properties but potential cognitive suppression. The reference compounds piracetam and fabomotizole exhibited limited efficacy, with piracetam potentially exacerbating certain anxiety parameters and fabomotizole showing only partial anxiolytic effects.

Study of Markers of Neuronal Damage

The experimental data presented in Figure 6 (Tables S4 and S5) provide valuable insights into the neurobiochemical changes induced by ketamine anesthesia and the potential neuroprotective effects of chosen two representatives, compounds **31** and **26**, compared to the reference drug piracetam.
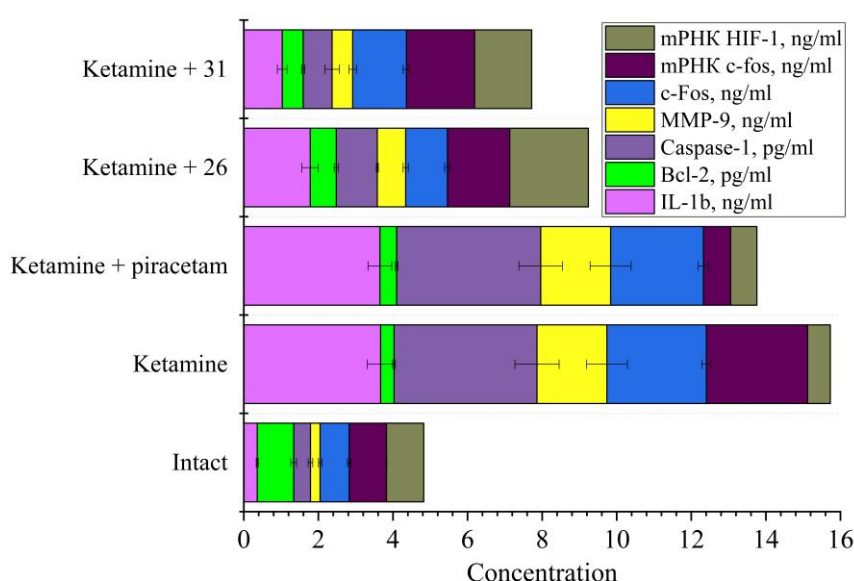
Figure 6. Neuroprotective effects of compounds on molecular markers and gene expression in rat brain following ketamine anesthesia. Effects on caspase-1 and Bcl-2 concentration in cytosolic fractions and on c-fos and HIF-1 mRNA expression in the CA1 hippocampal zone. Data for caspase-1 (pg/ml) and Bcl-2 (pg/ml) normalized by dividing by 100 for scale compatibility. Significant differences ($p<0.05$) compared to intact or control animals are indicated.

Inflammatory and apoptotic markers. Ketamine anesthesia significantly increased IL-1β concentration (approximately 11.8-fold) in the rat brain cytosolic fraction compared to intact animals. This substantial elevation indicates pronounced neuroinflammatory activation. Both compounds **31** and **26** demonstrated anti-inflammatory properties, reducing IL-1β levels by 72% and 51.5% respectively, compared to the control group. Notably, compound **31** showed superior anti-inflammatory efficacy. In contrast, piracetam failed to mitigate ketamine-induced IL-1β elevation, suggesting its limited anti-inflammatory capacity in this model.

The anti-apoptotic protein Bcl-2 was markedly reduced (by 63.4%) following ketamine administration, indicating compromised neuroprotective mechanisms. Both test compounds partially restored Bcl-2 levels, with compound **26** demonstrating greater efficacy (96.2% increase from control) compared to compound **31** (56.6% increase). Piracetam showed modest Bcl-2 restoration (25.1% increase), substantially less effective than the test compounds.

Inflammasome activation. Caspase-1, a key component of the inflammasome complex and indicator of pyroptotic cell death, was dramatically increased (8.5-fold) by ketamine anesthesia

(Figure 6). Compounds **31** and **26** significantly attenuated this elevation, reducing levels by 79.7% and 71.3% respectively, with compound **31** showing slightly superior efficacy. Piracetam showed no effect on caspase-1 levels, suggesting its inability to modulate inflammasome activation.

Matrix metalloproteinase and neuronal activation. MMP-9, associated with blood-brain barrier disruption and neuroinflammation, increased 7.2-fold following ketamine administration. Both test compounds reduced MMP-9 levels, though the reduction did not reach the intact animal baseline. Piracetam showed no effect on MMP-9 elevation.

The neuronal activation marker c-fos increased 3.4-fold with ketamine anesthesia. Compounds **31** and **26** reduced c-fos protein levels by 46.1% and 58.1% respectively, with compound **26** showing greater efficacy. Piracetam minimally affected c-fos protein levels.

Gene expression analysis. The mRNA expression data from the CA1 hippocampal region revealed interesting patterns. Ketamine increased c-fos mRNA expression 2.7-fold, consistent with the protein level findings. Compounds **31** and **26** partially normalized c-fos transcription, reducing it by 32.5% and 38.4% respectively. Interestingly, piracetam reduced c-fos mRNA below intact animal levels, suggesting potential transcriptional suppression, that did not translate to proportional protein reduction.

Hypoxia-inducible factor 1 (HIF-1) mRNA was reduced by 38.9% following ketamine administration, indicating impaired hypoxic adaptation. Both test compounds not only restored but significantly elevated HIF-1 mRNA levels above intact baselines. Compound **26** showed superior efficacy, increasing HIF-1 mRNA 3.5-fold compared to control. Piracetam showed minimal effect on its ketamine-induced reduction.

Comparative efficiency and mechanism implications. Overall, compounds **31** and **26** demonstrated substantial neuroprotective properties across multiple parameters compared to piracetam. Their efficacy profiles suggest following different mechanistic pathways.

Compound **31** showed superior anti-inflammatory and anti-inflammasome activity, suggesting potent modulation of innate immune responses in the brain. Compound **26** demonstrated stronger effects on anti-apoptotic protein restoration and HIF-1 expression, indicating potentially greater influence on cell survival pathways and hypoxic adaptation.

Piracetam showed limited efficacy across most parameters, with modest effects only on Bcl-2 levels and c-fos transcription, consistent with its known mild neuroprotective profile.

The differential regulation of HIF-1 by the test compounds is particularly noteworthy, as it suggests potential enhancement of adaptive hypoxic responses, that may confer broader neuroprotection beyond inflammatory modulation.

These findings should be considered within the context of several limitations. The acute nature of the model may not fully represent chronic ketamine exposure scenarios. Additionally, regional specificity beyond the CA1 hippocampal zone was not assessed. Future investigations should examine the dose-dependency of these effects and explore additional brain regions and cell-specific responses to better characterize the neuroprotective mechanisms of compounds **31** and **26**.

Nevertheless, our results are consistent with the scientific concept of CNS disruption following ketamine anesthesia. Ketamine-induced NMDA receptor hyperstimulation triggers excessive Ca^{2+} influx, initiating a cascade of pathological events including reactive oxygen species (ROS) formation, neuroinflammation, and neuroapoptosis [56,57]. This mechanism aligns with established literature demonstrating that ketamine anesthesia precipitates postoperative cognitive dysfunction (POCD), characterized by anxiety and cognitive impairments stemming from neuroapoptotic processes. Particularly compelling is the dose-dependent apoptotic neurodegeneration observed in immature mouse brains following ketamine exposure, suggesting developmental vulnerability to anesthetic neurotoxicity [58].

The neuroapoptotic pathway appears intricately linked to ketamine-induced c-fos expression across multiple brain regions. While NMDA receptor antagonism represents ketamine's primary mechanism of action, our findings support that ketamine-induced expression is mediated through additional pathways, notably sigma receptors. The complex pathogenesis of apoptosis in the nervous

system involves numerous signaling systems, with immediate early response genes (c-jun, c-fos) playing a critical role. The c-fos protein functions as a transcriptional regulator for multiple inducible genes, orchestrating cellular growth and differentiation processes, thereby serving as a recognized marker of neuronal activation [59].

Our previous investigations demonstrated a significant increase in c-fos-positive cell density within the CA1 hippocampal region following ketamine anesthesia [16]. The current findings of elevated c-fos mRNA expression in this region corroborate these observations and align with independent reports in the literature [60,61], establishing a consistent pattern of ketamine-induced neuronal activation in hippocampal structures critical for memory formation.

POCD pathophysiology extends beyond neuronal activation to include enhanced transcription and expression of proinflammatory cytokines TNF-α and IL-1β, alongside microglial activation within the hippocampus. This neuroinflammatory response likely contributes substantially to hippocampus-dependent memory impairment. Moreover, systemic inflammation appears to exacerbate cognitive dysfunction induced by surgical interventions [62], suggesting a bidirectional relationship between peripheral and central inflammatory processes.

A pivotal finding in our study concerns ketamine's enhancement of caspase-1 expression, which not only elevates TNF-α and IL-1β levels but also initiates pyroptosis - a distinct form of programmed cell death. Caspase-1-dependent pyroptosis emerges as a significant pathway involved in mitochondria-related apoptosis underlying ketamine-induced hippocampal neurotoxicity [63]. This mechanism may represent a critical convergence point between inflammatory and apoptotic processes in anesthetic-induced neurotoxicity.

Further exacerbating these pathological processes, ketamine-induced matrix metalloproteinase-9 (MMP-9) expression amplifies both neuroapoptosis and neuroinflammation, potentially through blood-brain barrier disruption [64]. Our compounds demonstrate efficacy in mitigating these neuroinflammatory effects associated with POCD and memory dysfunction.

The molecular basis of ketamine neurotoxicity further involves significant reduction in anti-apoptotic protein (Bcl-2) expression, increased pro-apoptotic protein Bax expression, and stimulated cytochrome-c release from mitochondria in primary cortical neurons [59]. Our investigation reveals that anesthetic-induced neuroapoptosis and cognitive dysfunction are associated with suppression of protective proteins HSP70 and HIF-1 expression [65], with decreased HIF-1 expression specifically documented in this study.

The neurobiochemical data presented above provides valuable mechanistic insights into the neuroprotective effects of our novel compounds. Ketamine anesthesia clearly induces a complex cascade of pathological events involving neuroinflammation, cell death pathways, and altered gene expression. Compounds **31** and **26** demonstrate distinct patterns of efficacy across these pathways, suggesting structure-dependent mechanisms of action. To better understand these structure-function relationships and inform future drug development efforts, we next conducted a comprehensive analysis of the structural features that drive the observed biological activities and efficacy profiles of compounds.

Structure-Activity Relationships

Correlation Molecular Structure and Behavioral Profiles

The results presented in the Table 4 reveal several found important structure-activity relationships among studied compounds in the post-ketamine anesthesia recovery model.

Influence of the Spiro-Junction Type

The spiro-junction (cyclohexane *vs.* *N*-methylpiperidine) appears to dictate not only behavioral outcomes but also specific neurobiochemical pathways:

Table 4. Structure-activity relationship of novel 6'*H*-spiro [cyclohexane/piperidine-1,5'/4,5'- [1,2,4]triazolo [1,5-*c*]quinazoline] derivatives in post-ketamine recovery model.

Sub.	Structural features	Behavioral profile	Key effects	Potential applications
25	spiro cyclohexane 2'-cyclopropyl 4-(*tert*-butyl)	Anti-hyperactivity	Normalized total activity Reduced high activity duration Increased low activity duration Normalized immobility Increased grooming behavior	Ketamine recovery Potential anxiolytic
26	spiro cyclohexane 2'-cyclohexyl 4-(*tert*-butyl)	Anti-hyperactivity	Normalized total activity Reduced high activity duration Normal low activity Reduced immobility Increased grooming behavior	Ketamine recovery Mild anxiolytic
31	spiro *N*-methyl-piperidine 2'-cyclopropyl	Stimulatory / Anxiolytic	Increased total activity Increased high activity duration Maximum center entries Increased distance traveled High free distance	Anxiolytic Potential anti-depressant Enhanced recovery
32	spiro *N*-methyl-piperidine 2'-cyclohexyl	Anti-hyperactivity	Normalized total activity Reduced high activity duration Normal low activity Increased grooming behavior	Ketamine recovery Anxiolytic
33	spiro *N*-methyl-piperidine 2'-adamantyl	Sedative-like	Moderately reduced activity Minimal center entries Highest immobility Reduced distance traveled Maintained elevated defecation	Sedative Potential hypnotic Different mechanism than traditional anxiolytics

Cyclohexane spiro-junction (compounds **25** and **26**) confers stabilizing effects on ketamine-induced behavioral alterations. Neurobiochemically, compound **26** demonstrated superior efficacy in Bcl-2 restoration and HIF-1 upregulation, suggesting that this structural element may preferentially modulate cell survival pathways and hypoxic adaptation mechanisms rather than direct anti-inflammatory actions.

N-methylpiperidine spiro-junction (compounds **31**, **32**, and **33**) yields diverse activity profiles that strongly depend on the 2'-substituent. The basic nitrogen atom in the piperidine ring may enhance compound **31**'s anti-inflammatory properties, as evidenced by its superior reduction of IL-1β and caspase-1 levels. This suggests that the *N*-methylpiperidine scaffold may facilitate interactions with inflammatory mediators or their regulatory pathways.

Impact of 2'-position substituents

The 2'-position substituent critically determines both behavioral and neurobiochemical profiles:

Cyclopropyl substitution: When combined with *N*-methylpiperidine (compound **31**), it produces stimulatory/anxiolytic effects behaviorally while demonstrating superior anti-inflammatory and anti-inflammasome activity. The compact, rigid cyclopropyl group may enhance binding to specific receptors or proteins involved in inflammatory cascades. In contrast, when paired with cyclohexane (**25**), it yields anti-hyperactivity effects, suggesting a complex interplay between this substituent and the spiro-junction type.

Cyclohexyl substitution: Derivatives with this moiety (compounds **26** and **32**) consistently normalize ketamine-induced hyperactivity regardless of the spiro-junction type. Notably, compound **26** demonstrated exceptional efficacy in restoring Bcl-2 levels and elevating HIF-1 mRNA expression, suggesting that the cyclohexyl group may optimize interactions with proteins involved in cell survival and hypoxic adaptation pathways.

Adamantyl substitution: The adamantyl-piperidine derivative (**33**) displays a unique sedative-like profile. While not directly examined in the neurobiochemical analyses, its structural properties suggest it may have distinct effects on neuronal signaling, possibly through enhanced blood-brain barrier penetration or interaction with sedation-mediating receptors.

Behavioral Markers and Neurobiochemical Correlates

Self-grooming behavior and neuroinflammation. Compounds **25**, **26**, and **32** significantly increased both short and extended grooming behaviors. Interestingly, compounds **26** and **31** (examined in the neurobiochemical analyses) both reduced IL-1β and caspase-1 levels, suggesting that attenuation of neuroinflammation might contribute to normalized grooming patterns. The differential effects on c-fos expression (with compound **26** showing greater reduction) may further explain the nuanced behavioral differences between these compounds.

Locomotor activity and HIF-1 expression. The normalization of locomotor activity observed with compound **26** correlates with its remarkable ability to upregulate HIF-1 mRNA. HIF-1 plays a critical role in neural adaptation to stress conditions, and its enhanced expression may contribute to improved behavioral recovery through optimized neuronal metabolism and resilience.

Structure-Based Optimization Strategies

Based on these integrated findings, we propose refined optimization strategies:

For anxiolytic compounds with anti-inflammatory properties, the cyclopropyl-piperidine scaffold (compound **31**) offers a promising starting point. Further modifications could enhance its anti-inflammatory potency while preserving its anxiolytic behavioral profile.

For neuroprotective agents that normalize ketamine-induced hyperactivity, the cyclohexyl derivatives (compounds **26** and **32**) provide excellent lead structures. Optimization efforts could focus on enhancing Bcl-2 restoration and HIF-1 upregulation while maintaining their behavioral benefits.

For dual-action compounds targeting both inflammation and apoptosis, hybrid structures incorporating features from both compounds **31** and **26** could yield candidates with complementary mechanisms of action.

For sedative compounds, the adamantyl-piperidine structure (compound **33**) could be further optimized, with additional investigation of its neurobiochemical profile to understand its mechanism of action.

Molecular Mechanisms and Target Hypotheses

The differential effects on inflammatory markers (IL-1β, caspase-1), apoptotic regulators (Bcl-2), and adaptive response factors (HIF-1) suggest multiple molecular targets for these compounds:

Compound **31**'s superior anti-inflammatory and anti-inflammasome activity suggests potential interaction with inflammasome components (NLRP3, ASC) or upstream regulators. Compound **26**'s pronounced effect on Bcl-2 and HIF-1 suggests possible modulation of mitochondrial function or hypoxia-sensing pathways. The differential effects on MMP-9 and c-fos indicate that these compounds may also influence neuronal activation and matrix remodeling processes. Importantly, the structure-activity relationships described here are based on binding affinity and behavioral outcomes. Future structure-function studies incorporating direct receptor activation/inhibition assays will be essential to correlate structural features with specific pharmacological mechanisms (agonism *vs.* antagonism *vs.* allosteric modulation).

The interplay between glutamatergic and GABAergic neurotransmission critically influences cognitive behaviors disrupted in POCD. Post-ketamine activation of specific GABAergic pathways beneficially impacts spontaneous motor behavior, environmental habituation, and spatial learning - core deficits in postoperative cognitive dysfunction. This suggests a potential shift in GABAergic signaling from receptor-mediated effects toward neurometabolic functions, particularly energy metabolism and mitochondrial processes [22,66–68].

Our data align with findings that modulation of serotonergic signaling - specifically 5-HT1A receptor blockade coupled with 5-HT2A receptor activation - reduces hippocampal apoptosis and attenuates anxiety, motor impairments, and environmental habituation deficits induced by various pharmacological agents [69,70]. The novel compounds investigated here, possessing affinity for GABA and specific serotonin receptor subtypes, appear to interrupt the cascade of adverse molecular and biochemical reactions following ketamine administration. This interruption attenuates excitotoxicity, neuroinflammation, neuroapoptosis, and reduced endogenous neuroprotection, thereby mitigating subsequent anxiety, irritability, spontaneous behavior impairments, and learning and memory deficits.

The comprehensive neuroprotective profile of compounds **31** and **26** against multiple ketamine-induced pathological processes presents promising therapeutic potential for preventing or treating anesthetic-induced neurocognitive dysfunction. Their differential mechanistic actions on inflammatory, apoptotic, and adaptive pathways warrant further investigation in diverse anesthetic exposure paradigms and potential clinical translation.

Further receptor binding and mechanistic studies would help elucidate the precise molecular targets responsible for these effects. This integrated structure-activity relationship analysis provides a rational basis for the design of novel 2'-R-6'*H*-spiro(cycloalkyl, heterocyclyl) [1,2,4]triazolo [1,5-*c*]quinazolines with targeted effects on specific neurobiochemical pathways. The identified patterns could guide the development of new therapeutic agents for managing ketamine anesthesia recovery or treating neuroinflammatory and anxiety-related conditions.

In Silico Molecular Docking to Nootropic and Anxiolytic Targets

Molecular Docking General Results

Three representative compounds were selected for in-depth investigation based on their distinctive structural features and pharmacological profiles: compounds **24** (2'-(pyridin-3-yl)-6'*H*-spiro [cyclohexane-1,5'- [1,2,4]triazolo [1,5-*c*]quinazoline]), **26** (spiro cyclohexane with 2'-cyclohexyl substitution), and **31** (spiro *N*-methylpiperidine with 2'-cyclopropyl substitution). This selection

encompasses compounds with demonstrated *in vivo* efficacy (**26** and **31**) and superior binding affinity to key receptors (**24**).

The following receptors represent major therapeutic targets across various neurological, psychiatric, and cardiovascular conditions, and were chosen as the targets. CB2 (5ZTY): Signal transduction and cell communication with roles in anxiety-like behaviors, particularly demonstrated in predator-induced fear models [34]. GABA(A)R $\alpha 1/\beta 3/\gamma 2L$ (6HUP): Major inhibitory neurotransmitter receptor involved in anxiety regulation, sleep regulation, and sedation, particularly relevant for trauma-related disorders [71]. M2 muscarinic acetylcholine receptor (5ZKB): Involved in memory, attention, and varios physiological functions as characterized in structural studies [27]. D2 dopamine receptor (6CM4): Critical for reward, motor control, and executive function, with structural insights informing therapeutic development [36]. Serotonin 1A (5-HT1A) receptor (8FYX): Key role in anxiety and depression regulation, with demonstrated anxiolytic effects in amygdala [35]. Serotonin 7 (5-HT7) receptor (7XTC): Involved in mood regulation and cognitive processes, characterized through selective antagonist studies [30]. CRF1R (4K5Y): Central to stress response and anxiety behaviors, with established pharmacological profiles in stress-related disorders [33]. Glutamate receptor 3 (GluA3) (3XSL): These receptors mediate fast excitatory synaptic transmission in the brain by allowing the influx of cations (primarily sodium and calcium) upon binding of the neurotransmitter glutamate [43]. mGluR5 (4OO9): Critical for synaptic plasticity and learning, with structural insights informing therapeutic development [31].

The molecular docking analyses reveal remarkable binding profiles across multiple neuronal targets (Figure 7, Table S6), providing mechanistic insights into the neurobiochemical and behavioral effects observed in previous studies.

Additionally, compounds demonstrated significant binding capacities beyond primary reference sites towards 8FYX, 7XTC, 4K5Y and 4OO9 (Figure 7, left panel, Table S7-S14), that differ from the reference ones, and had higher affinity value. This indicates specific structural complementarity to the primary binding sites while retaining flexibility for alternative binding modes.

Compound **26**: Balanced Multi-Target Engagement and Neuroprotection

The molecular docking results for compound **26** demonstrate balanced binding across multiple targets, with particularly strong affinity for the M2 muscarinic acetylcholine receptor (5ZKB, −10.7 kcal/mol) and GABA(A) receptor (6HUP, −10.4 kcal/mol). This multi-target engagement profile correlates with its comprehensive neuroprotective effects observed in neurobiochemical studies:
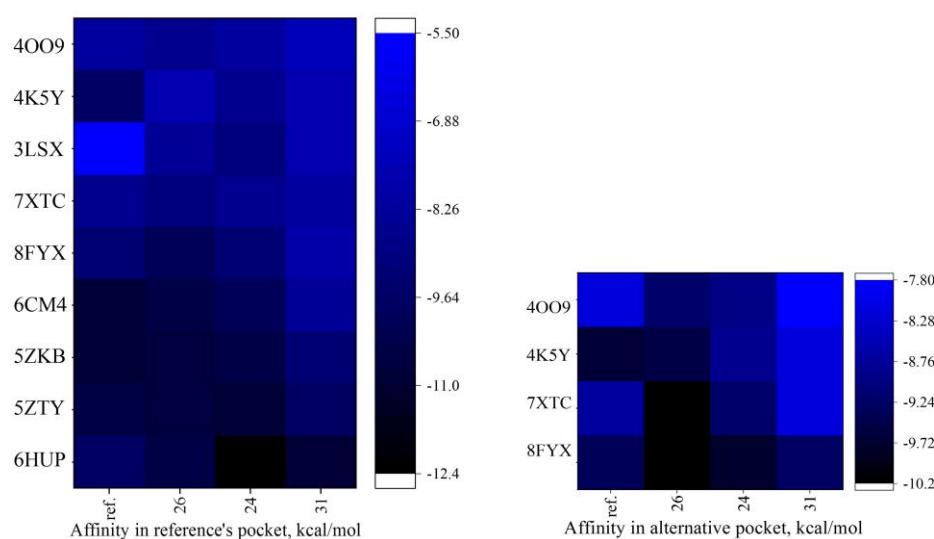
Figure 7. Binding affinities of compounds to nootropic and anxiolytic receptors. *Left panel*: Substance binding energies in reference's pocket (kcal/mol). *Right panel*: Substances best binding energies in alternative pockets

(kcal/mol). Color intensity indicates binding strength (darker = stronger binding). Target receptors (RCSB PDB IDs) / reference substance: 6HUP: α1/β3/γ2L GABA(A)R / diazepam; 5ZTY: G protein coupled receptor / JWH-133; 5ZKB: M2 muscarinic acetylcholine receptor / AFDX-384; 6CM4: D2 dopamine receptor / risperidone; 8FYX: serotonin 1A (5-HT1A) receptor-Gi1 protein / buspirone; 7XTC: serotonin 7 (5-HT7) receptor-Gs-Nb35 / SB-269970; 3XSL: glutamate receptor 3 (GluA3) / pramiracetam; 4K5Y: corticotropin-releasing factor receptor 1 (CRF1R) / CP-154,526; 4OO9: human class C GPCR metabotropic glutamate receptor 5 transmembrane domain / mavoglurant.

M2 muscarinic receptor binding and cognitive effects: The strong binding to M2 muscarinic receptors may contribute to the compound's ability to normalize ketamine-induced hyperactivity without excessive sedation. This cholinergic modulation could enhance cognitive recovery, consistent with **26**'s ability to normalize total activity and reduce high activity duration in behavioral studies.

GABA(A) receptor modulation and anti-anxiety effects: The substantial affinity for GABA(A) receptors suggests anxiolytic properties, which align with the increased grooming behavior observed in behavioral studies—a marker of reduced anxiety in rodents.

Multi-target engagement and HIF-1 upregulation: The balanced binding profile across serotonergic (8FYX, 7XTC) and glutamatergic (3LSX, 4OO9) targets may underlie the compound's remarkable ability to upregulate HIF-1 mRNA expression (3.5-fold increase compared to control). This molecular signature suggests activation of multiple complementary signaling pathways that converge on adaptive stress responses.

Bcl-2 restoration and receptor profile: The exceptional efficacy in restoring Bcl-2 levels (96.2% increase from control) correlates with the compound's strong binding to cannabinoid receptors (5ZTY, −10.6 kcal/mol), which have been implicated in cell survival pathways.

Compound **31**: Selective anti-inflammatory activity despite lower overall binding

Compound **31** consistently demonstrated lower binding affinities across most targets compared to compounds **24** and **26**. However, it exhibited remarkable anti-inflammatory and anxiolytic properties in neurobiochemical and behavioral studies. This apparent discrepancy provides important insights:

Moderate GABA(A) binding and anxiolytic effects: Despite lower binding affinity to GABA(A) receptors (6HUP, −10.8 kcal/mol) compared to compound **24**, compound **31** demonstrated pronounced anxiolytic-like effects behaviorally. This suggests its anxiolytic mechanism may involve pathways beyond direct GABA(A) modulation.

Anti-inflammatory prominence despite modest binding: Compound **31**'s superior anti-inflammatory properties (72% reduction in IL-1β levels) and potent anti-inflammasome activity (79.7% reduction in caspase-1) contrast with its more modest receptor binding profile. This suggests its primary mechanism may involve modulation of inflammatory signaling cascades downstream of receptor activation rather than direct receptor antagonism.

Stimulatory profile and receptor engagement: The stimulatory behavioral effects observed (increased high activity duration, maximum center entries) may relate to its moderate binding to dopamine D2 receptors (6CM4, −8.3 kcal/mol) and serotonin receptors, indicating a complex interplay between monoaminergic systems.

*Compound **24**: Strong GABA(A) affinity with potential cognitive enhancement*

While not directly evaluated in the neurobiochemical and behavioral studies, the molecular docking results for compound **24** reveal exceptional binding to GABA(A) receptors (6HUP, −12.4 kcal/mol), substantially exceeding the reference compound diazepam (−9.8 kcal/mol):

Superior GABA(A) binding: The exceptionally strong GABA(A) receptor affinity suggests potentially potent anxiolytic or sedative effects that warrant future behavioral evaluation.

Glutamate receptor engagement: Strong binding to glutamate receptor 3 (GluA3, 3LSX, −9.1 kcal/mol) substantially exceeding the reference pramiracetam (−5.5 kcal/mol) suggests potential cognitive enhancement capabilities.

Balanced multi-target profile: The strong binding across cannabinoid, muscarinic, and dopaminergic targets suggests a multi-modal mechanism of action that may provide cognitive enhancement without excessive sedation.

Following the quantitative assessment of binding affinities through molecular docking simulations, the three-dimensional visualization of protein-ligand complexes provides critical spatial insights not captured by numerical scores alone. These 3D representations elucidate key intermolecular interactions, including hydrogen bonding networks, hydrophobic contacts, and potential steric hindrances, thereby contextualizing the previously calculated binding energies within the framework of the binding pocket.

Structural Comparison and Binding Site Interactions

This comparative visualization (Figure 8, Table 5) demonstrates how subtle structural modifications to the triazoloquinazoline scaffold produce distinct receptor binding profiles and subsequent pharmacological effects, providing molecular insights into their mechanism of action and therapeutic potential.
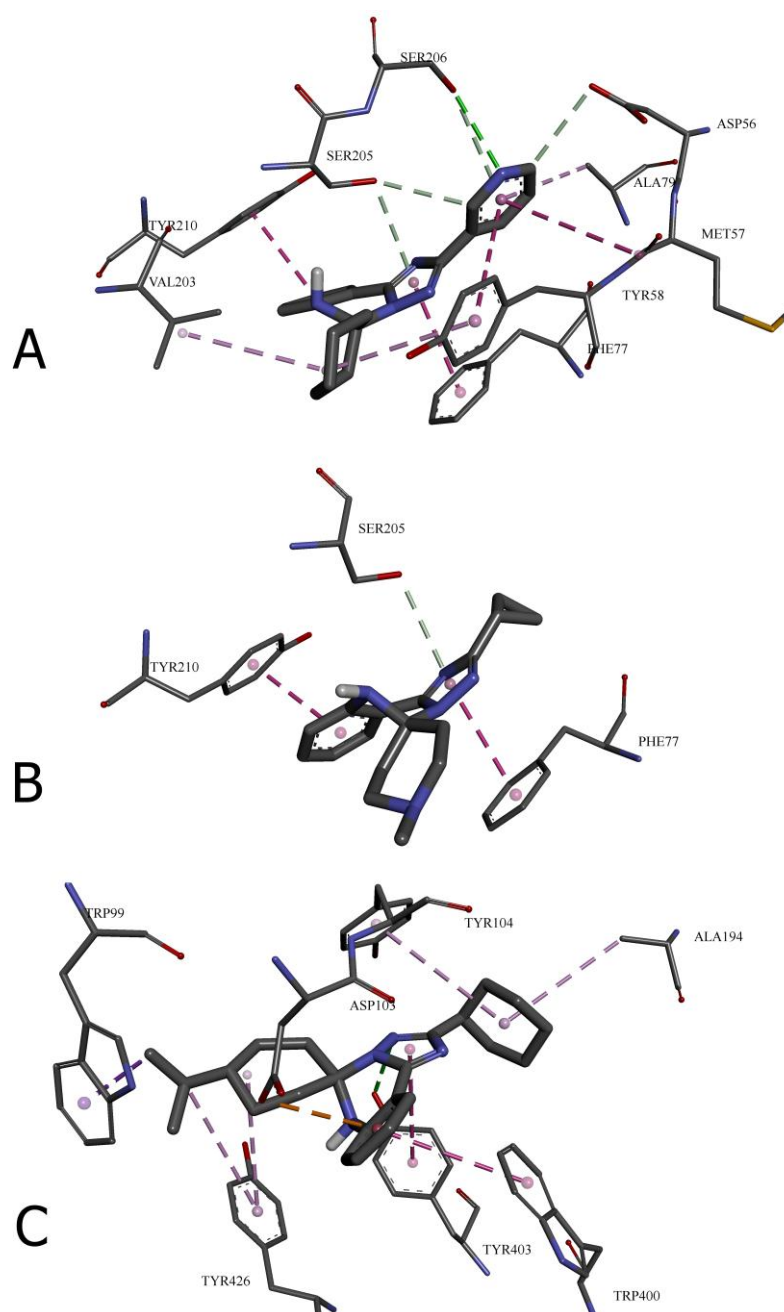
Figure 8. 3D visualization of molecular docking analyses of compounds **24**, **26**, and **31** with their primary receptor targets, highlighting different molecular interactions color-coded as follows: conventional hydrogen bonds (green), carbon hydrogen bonds and π-donor hydrogen bonds (light green), π-π stacked interactions, amide-π stacked and π-sigma interactions (purple), π-π T-shaped interactions (pink), alkyl, π-alkyl interactions (light pink), and electrostatic π-anion interactions (orange). *Panel A.* Compound **24** with GABA(A) receptor (PDB ID: 6HUP). *Panel B*. Compound **31** also with GABA(A) receptor (PDB ID: 6HUP). *Panel C.* Compound **26** with M2 muscarinic acetylcholine receptor (PDB ID: 5ZKB).

Panel A. The 2'-(pyridin-3-yl) derivative **24** demonstrates exceptional binding affinity (−12.4 kcal/mol) to the GABA(A) receptor, substantially exceeding the reference compound diazepam (−9.8 kcal/mol) [47]. This enhanced binding profile can be attributed to its diverse interaction network. The molecular interaction data reveals that compound **24** forms multiple hydrogen bonds with the receptor, including a strong conventional hydrogen bond with SER206 (3.09 Å), suggesting a key anchoring point for ligand recognition. Additionally, carbon hydrogen bonds with ASP56 and SER205 further stabilize the complex.

Table 5. Molecular interactions between novel compounds (**24**, **31**, and **26**) and neurotransmitter receptors: bond distances, categories, and types.

Amino acid residue	Distance, Å³	Bond category	Bond type
24 with GABA(A) receptor (6HUP)			
SER206	3.09118	Hydrogen Bond	Conventional Hydrogen Bond
ASP56	3.28520	Hydrogen Bond	Carbon Hydrogen Bond
SER205	3.28938	Hydrogen Bond	Carbon Hydrogen Bond
SER205	3.67482	Hydrogen Bond	π-Donor Hydrogen Bond
SER206	3.90775	Hydrogen Bond	π-Donor Hydrogen Bond
TYR58	5.76264	Hydrophobic	π-π Stacked
TYR210	4.04531	Hydrophobic	π-π Stacked
PHE77	4.01868	Hydrophobic	π-π Stacked
MET57	5.04132	Hydrophobic	Amide-π Stacked
VAL203	4.58572	Hydrophobic	Alkyl
TYR58	4.92210	Hydrophobic	π-Alkyl
ALA79	4.92852	Hydrophobic	π-Alkyl
31 with GABA(A) receptor (6HUP)			
SER205	3.75260	Hydrogen Bond	π-Donor Hydrogen Bond
PHE77	3.96894	Hydrophobic	π-π Stacked
TYR210	3.99648	Hydrophobic	π-π Stacked
26 with M2 muscarinic acetylcholine receptor (5ZKB)			
TYR403	2.87801	Hydrogen Bond	Conventional Hydrogen Bond
ASP103	3.70202	Electrostatic	π-Anion
TRP99	3.93043	Hydrophobic	π-Sigma
TRP400	4.88215	Hydrophobic	π-π T-shaped
TYR403	5.01930	Hydrophobic	π-π T-shaped
ALA194	4.93091	Hydrophobic	Alkyl
TYR104	5.41339	Hydrophobic	π-Alkyl

TYR426	5.13581	Hydrophobic	π-Alkyl
TYR426	5.27219	Hydrophobic	π-Alkyl

*Bond distances are reported in Angstroms (Å) and represent the shortest atomic distance between the interacting groups. Smaller distances generally indicate stronger interactions, particularly for hydrogen bonds where distances below 3.0 Å typically represent strong binding. Hydrogen bonds are classified into conventional, carbon hydrogen, and π-donor types based on the interacting atoms and their geometrical orientation. Conventional hydrogen bonds typically involve electronegative atoms (O, N) as acceptors. Hydrophobic interactions are categorized as π-π stacked, π-π T-shaped, amide-π stacked, alkyl, and π-alkyl based on the relative orientation of aromatic rings and aliphatic groups. The electrostatic π-anion interaction observed between compound **26** and ASP103 of the M2 receptor involves negatively charged carboxylate groups interacting with the electron-rich π system of the ligand. These molecular interactions contribute to the binding affinity and specificity of the compounds for their respective receptors, potentially correlating with their pharmacological activities.

The interaction profile is notably enriched by extensive hydrophobic contacts, particularly π-π stacked interactions with TYR58, TYR210, and PHE77. These aromatic interactions likely contribute significantly to the compound's high binding affinity by providing optimal spatial orientation within the binding pocket. The presence of both hydrogen bonding and hydrophobic interactions creates a complementary binding mechanism that explains the substantially higher affinity compared to diazepam.

Panel B. Compound **31**, the *N*-methylpiperidine spiro derivative with 2'-cyclopropyl substitution, displays moderate binding affinity (−10.8 kcal/mol) to the GABA(A) receptor, also exceeding the reference compound diazepam. Its interaction profile appears more selective, primarily featuring a π-donor hydrogen bond with SER205 (3.75 Å) and prominent π-π stacked hydrophobic interactions with PHE77 and TYR210.

The reduced number of interactions compared to compound **24** correlates with its moderately lower binding affinity, suggesting that the cyclopropyl moiety provides sufficient but not optimal receptor engagement. Notably, both compounds **24** and **31** interact with similar residues (SER205, PHE77, TYR210), indicating a common binding mode at the GABA(A) receptor despite their structural differences.

Panel C. Compound **26**, the 2'-cyclohexyl derivative, demonstrates strong binding (−10.7 kcal/mol) to the M2 muscarinic receptor, comparable to the reference antagonist AFDX-384 (−10.9 kcal/mol). Its interaction profile differs significantly from the GABA(A)-binding compounds, highlighting receptor selectivity among these derivatives.

The strong conventional hydrogen bond with TYR403 (2.88 Å) appears to be a critical anchoring point for recognition at the M2 receptor. Uniquely, compound **26** exhibits an electrostatic π-anion interaction with ASP103, not observed with the other compounds. This electrostatic component likely contributes significantly to its binding specificity for the M2 receptor.

The hydrophobic interaction network is also distinctive, featuring π-sigma interaction with TRP99 and π-π T-shaped interactions with TRP400 and TYR403, instead of the π-π stacked interactions observed with GABA(A) receptor binders. The different geometrical orientation of these hydrophobic contacts suggests receptor-specific spatial accommodation of the cyclohexyl moiety.

The predominance of aromatic interactions across all compounds highlights the importance of the triazoloquinazoline core scaffold in receptor recognition.

Integrated Structure-Activity Relationships

Analysis of molecular docking results with previous neurobiochemical and behavioral findings reveals comprehensive structure-activity relationships:

Spirocyclic core determinants. Cyclohexane-based spirocycles (compounds **24** and **26**) generally confer stronger receptor binding affinities than the *N*-methylpiperidine spirocycle (compound **31**). However, the *N*-methylpiperidine in compound **31** appears to enhance anti-inflammatory properties

despite reduced receptor binding, suggesting this structural element may influence signaling cascades beyond direct receptor interaction. The cyclohexane spirocycle in compound **26** facilitates balanced receptor engagement while promoting Bcl-2 restoration and HIF-1 upregulation, indicating enhanced neuroprotective capabilities.

Pyridin-3-yl substituent (**24**). Substantially enhances GABA(A) receptor binding, suggesting strong anxiolytic potential. Improves glutamate receptor binding, indicating possible cognitive enhancement properties. The nitrogen-containing aromatic ring likely forms additional hydrogen bonds within binding pockets.

Cyclohexyl substituent (**26**). Provides balanced binding across multiple targets, correlating with its comprehensive neuroprotective profile. The conformational flexibility of the cyclohexyl group may allow adaptable binding to diverse receptor architectures. This structural feature appears optimal for HIF-1 upregulation and Bcl-2 restoration, suggesting enhanced cell survival mechanism engagement.

Cyclopropyl substituent (**31**). Less favorable for direct receptor binding, particularly at dopamine and serotonin receptors. However, this structural feature appears to enhance anti-inflammatory and anti-inflammasome activity, suggesting specific interactions with inflammatory pathways. The compact, rigid cyclopropyl group may facilitate interactions with specific modulators of inflammatory cascades rather than neurotransmitter receptors.

Mechanistic Framework and Polypharmacology

The integration of molecular docking, neurobiochemical, and behavioral data suggests a complex mechanistic framework for these compounds:

Multi-target engagement hypothesis. The balanced binding profiles suggest synergistic positive modulation across multiple receptors rather than broad-spectrum antagonism. This enhancement-based multi-target strategy aligns with contemporary understanding that cognitive improvement requires coordinated activation of complementary pathways rather than neurotransmitter blockade, and than strong interaction with a single receptor type, as highlighted by Jędrejko *et al.* [46].

Divergent primary mechanisms. Compound **26** appears to function primarily through enhanced cell survival pathways (Bcl-2 restoration) and adaptive responses (HIF-1 upregulation), facilitated by balanced receptor engagement. Compound **31** primarily modulates inflammatory pathways (IL-1β and caspase-1 reduction) with moderate receptor interaction, suggesting its mechanism involves signaling cascades downstream of receptor activation. Compound **24**'s strong GABA(A) and glutamate receptor binding suggests direct neurotransmitter system modulation as its primary mechanism.

Structure-dependent signaling pathway activation. Cyclohexane spirocycle + cyclohexyl substituent (**26**): preferentially activates cell survival and hypoxic adaptation pathways. *N*-methylpiperidine spirocycle + cyclopropyl substituent (**31**): primarily modulates inflammatory signaling cascades. Cyclohexane spirocycle + pyridin-3-yl substituent (**24**): directly modulates inhibitory and excitatory neurotransmission.

Therapeutic Implications and Optimization Strategies

This Integrated Analysis Provides Rational Guidance for Therapeutic Applications and Further Optimization:

Target-specific compound selection. For anti-anxiety applications with mild sedation: compound **24** (strongest GABA(A) binding). For neuroprotection with balanced cognitive effects: compound **26** (optimal Bcl-2 and HIF-1 modulation). For anti-neuroinflammatory applications with anxiolytic properties: compound **31** (superior anti-inflammatory profile)

Structural optimization approaches. For enhanced GABA(A) binding: incorporate pyridin-3-yl substituent at 2'-position. For balanced neuroprotection: utilize cyclohexyl substituent at 2'-position

with cyclohexane spirocycle. For anti-inflammatory potency: explore modifications of the cyclopropyl-piperidine scaffold.

Hybrid compound development. Compounds incorporating features of both **26** and **31** might yield candidates with dual neuroprotective and anti-inflammatory properties. Hybrids of **24** and **26** could enhance both direct GABA(A) modulation and cell survival pathway activation.

Future Research Directions

This integrated analysis suggests several promising research directions:

Receptor binding assays. Experimental validation of the computational docking predictions through radioligand binding studies to confirm target engagement. Future studies should include:

- Patch-clamp electrophysiology to confirm GABA(A) positive allosteric modulation *vs.* direct agonism
- Calcium imaging assays to verify glutamate receptor enhancement *vs.* inhibition
- cAMP functional assays for serotonin receptor activity (agonist *vs.* antagonist classification)
- Receptor activation/inhibition dose-response curves to definitively establish functional mechanisms
- Competitive binding studies to distinguish allosteric *vs.* orthosteric site interactions
- Functional selectivity assessment to determine if compounds exhibit biased signaling at different receptor subtypes
- Allosteric *vs.* orthosteric binding determination through competitive displacement studies with known ligands
- Tissue-specific functional validation to account for potential regional differences in receptor expression and coupling

Pathway-specific investigations. Examination of the effects of these compounds on specific signaling pathways, particularly inflammasome components, HIF-1 regulatory mechanisms, and Bcl-2 associated proteins.

Structure-based design. Utilization of the identified structure-activity relationships to design next-generation compounds with enhanced target selectivity or multi-target profiles.

Extended behavioral evaluation. Comprehensive behavioral assessment of compound **24** to validate its predicted anxiolytic potential based on exceptional GABA(A) binding.

Dose-response relationships. Investigation of dose-dependent effects on receptor binding, neurobiochemical markers, and behavioral outcomes to establish optimal therapeutic windows.

This integrated framework of molecular docking, neurobiochemical, and behavioral profiles provides a comprehensive understanding of these novel triazoloquinazoline derivatives, establishing a rational foundation for their further development as therapeutic agents for neuropsychiatric applications.

Limitations of the Study

This study represents a focused and strategic approach to evaluating the neuroprotective potential of novel compounds in a ketamine-induced model of cognitive impairment. By conducting *in vivo* assessments at a single dose, we established a clear baseline of efficacy, laying the groundwork for future dose-response studies that will define therapeutic windows and optimize treatment regimens.

Our emphasis on acute responses to ketamine administration allowed us to capture the early neurochemical and behavioral changes, providing critical insight into the immediate mechanisms of action. This acute-phase focus offers a foundation for future longitudinal studies aimed at exploring sustained and long-term neuroprotective effects.

We successfully identified transcriptional changes in key markers such as c-fos and HIF-1, offering valuable molecular insights into the treatment effects. Although protein-level validation *via* Western blotting was beyond the current study's scope, our findings provide a solid rationale for

future investigations into downstream translational events, including comprehensive proteomic profiling.

By proceeding directly to *in vivo* models, we prioritized physiological relevance and translational potential, enabling a realistic assessment of therapeutic outcomes. The use of a well-established ketamine-induced cognitive impairment model offers a focused and reliable platform to detect neuroprotective effects. This approach paves the way for expanding future research into other models of cognitive dysfunction, increasing the generalizability of findings.

Despite modest sample sizes (n = 6–10 per group), our results demonstrated consistent trends across behavioral and biochemical endpoints, suggesting meaningful biological effects. These findings justify larger-scale studies to further delineate subtle but potentially significant benefits.

The neurobiochemical analysis targeted well-characterized markers of inflammation, apoptosis, and neuroplasticity (e.g., IL-1β, Bcl-2, caspase-1, MMP-9, c-fos, HIF-1), providing mechanistic insight into the compounds' effects. While not exhaustive, this focused panel enables a clearer interpretation of specific pathways, which can be expanded in future research to encompass broader molecular networks.

Pharmacokinetic considerations were addressed through in silico predictions of blood-brain barrier permeability and metabolic stability, offering an efficient early assessment of drug-likeness and guiding compound selection for in vivo testing. These findings establish a strong starting point for future empirical validation.

We also provided preliminary binding affinity predictions, highlighting potential target interactions. Although functional receptor profiling remains to be conducted, the observed behavioral improvements suggest meaningful neuroactive engagement. These encouraging results support further work involving electrophysiological and biochemical assays to fully elucidate receptor dynamics and modulatory mechanisms.

Finally, the behavioral outcomes, assessed via the open field test in adult male rats, captured key locomotor and anxiety-related phenotypes. While this represents a controlled and standardized approach, it also opens avenues for future research to incorporate additional behavioral paradigms, developmental stages, and sex-based comparisons, thereby enhancing the translational relevance to diverse clinical populations.

Materials and Methods

Molecular Docking

CB-Dock2 [45,72], a protein-ligand auto blind docking tool, that inherits the curvature-based cavity detection procedure with AutoDock Vina, was used for calculations of tested substances' affinity to 10 macromolecules from RCSB Protein Data Bank, namely 5ZTY [34,73], 6HUP [71,74], 5ZKB [27,75], 6CM4 [36,76], 8FYX [35,77], (7XTC [30,78], 3LSX [43,79], 4K5Y [33,80], and 4OO9 [31,81] (Supplementary Materials, Table S1, S2, S6-S14). And the following substances (Figure 1) were used as the references: JWH-133: (6*aR*,10*aR*)-6,6,9-trimethyl-3-(2-methylpentan-2-yl)-6*a*,7,10,10*a*-tetrahydrobenzo [*c*]-chromene; diazepam: 7-chloro-1-methyl-5-phenyl-3*H*-1,4-benzodiazepin-2-one; AFDX-384: *N*- [2- [2- [(dipropylamino)methyl]piperidin-1-yl]ethyl]-6-oxo-5*H*-pyrido [2,3-*b*] [1,4]benzodiazepine-11-carboxamide; etrumadenant: 3- [2-amino-6- [1- [[6-(2-hydroxypropan-2-yl)pyridin-2-yl]methyl]-triazol-4-yl]pyrimidin-4-yl]-2-methylbenzonitrile; risperidone: 3- [2- [4-(6-fluoro-1,2-benzoxazol-3-yl)piperidin-1-yl]ethyl]-2-methyl-6,7,8,9-tetrahydropyrido [1,2-*a*]pyrimidin-4-one; buspirone: 8- [4-(4-pyrimidin-2-ylpiperazin-1-yl)butyl]-8-azaspiro [4.5]decane-7,9-dione; SB-269970: 3- [[(2*R*)-2- [2-(4-methyl-1-piperidinyl)ethyl]-1-pyrrolidinyl]sulfonyl]phenol; pramiracetam: *N*- [2- [di(propan-2-yl)amino]ethyl]-2-(2-oxopyrrolidin-1-yl)acetamide; CP-154,526: *N*-butyl-*N*-ethyl-2,5-dimethyl-7-(2,4,6-trimethylphenyl)-7*H*-pyrrolo [3,2-*e*]pyrimidin-4-amine; mavoglurant: methyl (3*aR*,4*S*,7*aR*)-4-hydroxy-4- [(3-methylphenyl)ethynyl]octahydro-1*H*-indole-1-carboxylate.

Synthesis

Melting points were measured in open capillary tubes using a «Mettler Toledo MP 50» apparatus (Columbus, USA). Elemental analyses (C, H, N) were conducted on an ELEMENTAR vario EL cube analyzer (Langenselbold, Germany), with the results for elements or functional groups de*via*ting by no more than ± 0.3% from the theoretical values. The ^{1}H and ^{13}C NMR spectra (500 MHz) were obtained on a Varian Mercury 500 spectrometer (Varian Inc., Palo Alto, CA, USA), using TMS as an internal standard in a DMSO-*d6* solution. LC-MS data were acquired using a chromatography/mass spectrometric system comprising the high-performance liquid chromatography «Agilent 1100 Series» (Agilent, Palo Alto, CA, USA) equipped with a diode-matrix detector and mass-selective detector, «Agilent LC/MSD SL» (Agilent, Palo Alto, USA), with atmospheric pressure chemical ionization (APCI).

The starting substances **a** were obtained according to the previously described method and physicochemical constants that correspond to the literature data [41,82]. Synthetic studies (Figure 3) were carried out according to general approaches using reagents from «Merck» (Darmstadt, Germany), «Sigma-Aldrich» (Missouri, USA) and «Enamine» (Kyiv, Ukraine).

General procedure for the synthesis of 2′-R-6'*H*-spiro(cycloalkyl-,heterocyclyl) [1,2,4]triazolo [1,5-*c*]quinazolines (**1-40**):

To a solution of 10 mmol of the corresponding [2-(3-R-1*H*-1,2,4-triazolo-5-yl)phenyl]amine (**a**) in 10 ml of propanol-2 (or ethanol, propanol-1) was added 10 mmol of the corresponding ketone (cyclobutanone, cyclopentanone, cyclohexanone, 4-(*tert*-butyl)cyclohexan-1-one, 1-methyl-piperidone-4) and 2 drops of concentrated sulfate acid. The reaction mixture is left at room temperature for 24 hours (method A) or boiled for up to 6 hours (method B). Cool, pour into a 10% sodium acetate solution. The resulting precipitate is filtered and dried. Crystallize from methanol if necessary.

Synthesized compounds are white crystalline substances insoluble in water, soluble in alcohols, dioxane and DMF. Spectral data are found in the Supplementary Materials.

Toxicity Studies

A virtual lab of website ProTox-II was used for the prediction toxicities of molecules [51,83]. It incorporates molecular similarity, fragment propensities, most frequent features and (fragment similarity-based CLUSTER cross-validation) machine-learning, based a total of 33 models for the prediction of various toxicity endpoints such as acute toxicity, hepatotoxicity, cytotoxicity, carcinogenicity, mutagenicity, immunotoxicity, adverse outcomes (Tox21) pathways and toxicity targets. All methods, statistics of training set as well as the cross-validation results can be found at their website.

SwissADME Analysis

The SwissADME virtual laboratory was utilized to calculate the physicochemical descriptors and predict the ADME parameters, pharmacokinetic properties and drug-likeness [52,84]. The fundamental approaches and methodology underlying SwissADME, a free web-based tool designed for evaluating pharmacokinetics and drug-likeness, are detailed in the scientific literature.

Biological Assay

Scope and Clinical Focus

This study primarily addresses POCD following ketamine anesthesia, with mechanistic insights potentially applicable to broader cognitive disorders. While PTSD-related pathways are discussed for mechanistic context, POCD represents our primary therapeutic target and validation model.

Rationale for Individual Compound Selection

Compound **25**: Selected as cyclohexane-spiro/cyclopropyl prototype with optimal safety profile (no cytotoxicity predictions) and enhanced lipophilicity from *tert*-butyl substitution. Compound **26**:

Chosen to evaluate cyclohexyl substitution effects on neuroprotection, representing the balanced multi-target engagement hypothesis with strong M2 muscarinic and GABA(A) binding. Compound **31**: Selected as the *N*-methylpiperidine archetype to assess anti-inflammatory potential, based on moderate GABA(A) binding (−10.8 kcal/mol) but distinct structural scaffold. Compound **32**: Included to directly compare cyclohexyl effects across different spiro-junction types (piperidine *vs*. cyclohexane framework). Compound **33**: Chosen to evaluate adamantyl substitution effects on CNS penetration and activity, representing the most lipophilic variant with unique pharmacokinetic properties. Compound **24**: Despite superior GluA3 binding affinity (−9.1 kcal/mol), compound **24** was excluded from *in vivo* studies due to: (1) structural similarity to compound **33** (both pyridine-containing), (2) resource limitations requiring strategic compound selection, and (3) prioritization of compounds with more balanced safety-efficacy profiles. Compound **24** remains a priority candidate for future investigation.

Animals

The studies were performed on a total of 54 rats (n = 6 intact, 6 control, and 42 experimental rats divided into groups III-IX), and all manipulations were carried out in accordance with the regulation on the use of animals in biomedical experiments (Council Directive 86/609/EEC) and the "General Ethical Principles of Animal Experiments" (EEC (1986). (Directive 2010/63/EU). The ZSMPhU Commission on Bioethics decided to adopt the experimental study protocols and outcomes (Protocol № 3, dated March 22, 2024). The design, execution, analysis, and reporting of the animal experiments in this study adhere to the Animal Research: Reporting of *In vivo* Experiments (ARRIVE) guidelines (Supplementary Material).

Statistical Analysis

Experimental data were statistically analyzed using "StatisticaR for Windows 6.0" (StatSoft Inc., Tulsa, OK, USA, AXXR712D833214FAN5), "SPSS16.0", and "Microsoft Office Excel 2010" software. Prior to statistical tests, we checked the results for normality (Shapiro–Wilk and Kolmogorov–Smirnov tests). In the normal distribution, intergroup differences were considered statistically significant based on the parametric Student's t-test. If the distribution was not normal, the comparative analysis was conducted using the non-parametric Mann–Whitney U-test. To compare independent variables in more than two selections, we applied ANOVA dispersion analysis for the normal distribution and the Kruskal–Wallis test for the non-normal distribution. To analyze correlations between parameters, we used correlation analysis based on the Pearson or Spearman correlation coefficient. For all types of analysis, the differences were considered statistically significant at $p < 0.05$ (95%).

Conclusions

This study demonstrates that novel 2'-R-6'*H*-spiro(cycloalkyl-,heterocyclyl) [1,2,4]triazolo [1,5-*c*]quinazolines represent promising neuroprotective agents for ketamine-induced cognitive dysfunction. Through integrated computational design, synthesis, and biological evaluation, compounds **25**, **26**, and **32** showed superior efficacy compared to piracetam and fabomotizole in normalizing behavioral parameters and reducing anxiety.

Molecular docking revealed significant multi-target binding affinities, particularly for glutamate receptor GluA3, exceeding reference compounds. ADMET evaluations confirmed favorable drug-likeness and safety profiles. Neurobiochemical *in vivo* studies demonstrated that compound **31** exhibits superior anti-inflammatory properties while **26** enhances cell survival pathways through Bcl-2 restoration and HIF-1 upregulation.

Structure-activity analyses established that cyclohexane spirocycles (**25**, **26**) normalize behavior while *N*-methylpiperidine derivatives (**31-33**) show diverse profiles dependent on 2'-substituents. Cyclohexyl substitution normalizes hyperactivity, whereas cyclopropyl-*N*-methylpiperidine

provides anxiolytic and anti-inflammatory effects. While behavioral evidence suggests positive receptor modulation rather than antagonism, definitive pharmacological classification requires functional validation studies.

These compounds effectively attenuate neuroinflammation, reduce caspase-1-mediated pyroptosis, and restore neuroprotective mechanisms, addressing ketamine neurotoxicity through multifaceted pathways. This work establishes spirotriazoloquinazolines as a valuable structural class with primary applications in ketamine-induced cognitive dysfunction and potential extension to related neuropsychiatric conditions. Future research should focus on lead optimization, mechanistic validation through receptor binding studies, and evaluation in diverse neurological models.

responsibility for the content of the publication; "II European Chemistry School for Ukrainians" (https://acmin.agh.edu.pl/en/detail/s/ii-european-chemistry-school-for-ukrainians) for scientific inspiration.

References

1. Leslie E, Pittman E, Drew B, Walrath B. Ketamine Use in Operation Enduring Freedom. Mil Med 2021;186:e720-e725.
2. Butler FK. Tactical Combat Casualty Care: Beginnings. Wilderness Environ Med 2017;28:S12-S17.
3. Barr J, Fraser GL, Puntillo K, Ely EW, Gélinas C, Dasta JF, Davidson JE, Devlin JW, Kress JP, Joffe AM, et al. Clinical practice guidelines for the management of pain, agitation, and delirium in adult patients in the intensive care unit. Crit Care Med 2013;41:263-306.
4. Cohen B, Talmy T, Gelikas S, Radomislensky I, Kontorovich-Chen D, Cohen B, Bar-Or D, Almog O, Glassberg E. Opioid sparing effect of ketamine in military prehospital pain management-A retrospective study. J Trauma Acute Care Surg 2022;93:S71-S77.
5. Riccardi A, Guarino M, Serra S, Spampinato MD, Vanni S, Shiffer D, Voza A, Fabbri A, De Iaco F. Low-Dose Ketamine for Pain Management. J Clin Med 2023;12:3256.
6. Li L, Vlisides PE. Ketamine: 50 Years of Modulating the Mind. Front Hum Neurosci 2016;10:612.
7. Hashimoto K. Detrimental Side Effects of Repeated Ketamine Infusions in the Brain. Am J Psychiatry 2016;173:1044-1045.
8. Pereira H, Antunes MV, Teles D, Pereira LG, Abelha F. Association between intraoperative ketamine and the incidence of emergence delirium in laparoscopic surgeries: an observational study. Braz J Anesthesiol 2024;74:744414.
9. Viderman D, Aubakirova M, Nabidollayeva F, Yegembayeva N, Bilotta F, Badenes R, Thorat AA, Yeseuleukova S, Baynazar D, Yerkinova A, et al. Effect of Ketamine on Postoperative Neurocognitive Disorders: A Systematic Review and Meta-Analysis. J Clin Med 2023;12:4314.
10. Belenichev I, Burlaka B, Puzyrenko A, Ryzhenko O, Kurochkin M, Yusuf J. Management of amnestic and behavioral disorders after ketamine anesthesia. Georgian Med News 2019;294:141-145.
11. Chen M, Han Y, Que B, Zhou R, Gan J, Dong X. Prophylactic Effects of Sub-anesthesia Ketamine on Cognitive Decline, Neuroinflammation, and Oxidative Stress in Elderly Mice. Am J Alzheimers Dis Other Demen 2022;37.
12. Ma J, Wang F, Wang J, Wang P, Dou X, Yao S, Dong X, Luo J. The Effect of Low-Dose Esketamine on Postoperative Neurocognitive Dysfunction in Elderly Patients Undergoing General Anesthesia for Gastrointestinal Tumors: A Randomized Controlled Trial. Drug Des Devel Ther 2023;17:1945-1957.
13. Lee KH, Kim JY, Kim JW, Park JS, Lee KW, Jeon SY. Influence of Ketamine on Early Postoperative Cognitive Function After Orthopedic Surgery in Elderly Patients. Anesth Pain Med 2015;5:e28844.
14. Haller G, Chan MTV, Combescure C, Lopez U, Pichon I, Licker M, Baele P, Bailie R, de Haever G, Ellerkmann R, et al. The international ENIGMA-II substudy on postoperative cognitive disorders (ISEP). Sci Rep 2021;11:11631.
15. Fang Y, Qiu Z, Hu W, Yang J, Yi X, Huang L, Zhang S. Effect of piracetam on the cognitive performance of patients undergoing coronary bypass surgery: A meta-analysis. Exp Ther Med 2014;7:429-434.
16. Belenichev IF, Burlaka BS, Ryzhenko OI, Ryzhenko VP, Aliyeva OG, Makyeyeva LV. Neuroprotective and anti-apoptotic activity of the IL-1 antagonist RAIL-gel in rats after ketamine anesthesia. Pharmakeftiki 2021;33:97-106.
17. Belenichev I, Popazova O, Bukhtiyarova N, Savchenko D, Oksenych V, Kamyshnyi O. Modulating Nitric Oxide: Implications for Cytotoxicity and Cytoprotection. Antioxidants 2024;13:504.
18. Usenko L, Krishtafor A, Polinchuk I, Tiutiunnik A, Usenko A, Petrashenok Y. Postoperative Cognitive Dysfunction as a Complication of General Anesthesia. The Importance of Early Pharmacological Neuroprotection. Emergency Medicine 2015;2:24-31.
19. Colucci L, Bosco M, Rosario Ziello A, Rea R, Amenta F, Fasanaro AM. Effectiveness of nootropic drugs with cholinergic activity in treatment of cognitive deficit: a review. J Exp Pharmacol 2012;4:163-172.

20. Dirks B, Seibert A, Sperling G, Krieglstein J. Vergleich der Wirkungen von Piracetam und Methohexital auf den zerebralen Energiestoffwechsel [Comparison of the effects of piracetam and methohexital on cerebral energy metabolism]. Arzneimittelforschung 1984;34:258-266.

21. Belenichev I, Gorchakova N, Kuchko*v*skyi O, Ryzhenko V, Varavka I, Varvanskyi P, Levchenko K, Yusuf J. Principles of metabolithotropic therapy in pediatric practice. Clinical and pharmacological characteristics of modern metabolithotropic agents (part 2). Phytother J 2022;4:5-29.

22. Belenichev I, Popazova O, Bukhtiyarova N, Ryzhenko V, Pavlov S, Suprun E, Tykhomyrov A, Zadoya A, Kaplaushenko A, Belenichev I, et al. Targeting Mitochondrial Dysfunction in Cerebral Ischemia: Advances in Pharmacological Interventions. Antioxidants 2025;14:108.

23. Sarawagi A, Soni ND, Patel AB. Glutamate and GABA Homeostasis and Neurometabolism in Major Depressive Disorder. Front Psychiatry 2021;12:637863.

24. Aznar S, Hervig MS. The 5-HT2A serotonin receptor in executive function: Implications for neuropsychiatric and neurodegenerative diseases. Neurosci Biobehav Rev 2016;64:63-82.

25. Sheng JA, Bales NJ, Myers SA, Bautista AI, Roueinfar M, Hale TM, Handa RJ. The Hypothalamic-Pituitary-Adrenal Axis: Development, Programming Actions of Hormones, and Maternal-Fetal Interactions. Front Behav Neurosci 2021;14:601939.

26. Smith C, Gentleman SM, Leclercq PD, Murray LS, Griffin WS, Graham DI, Nicoll JA. The neuroinflammatory response in humans after traumatic brain injury. Neuropathol Appl Neurobiol 2013;39:654-666.

27. Suno R, Lee S, Maeda S, Yasuda S, Yamashita K, Hirata K, Horita S, Tawaramoto MS, Tsujimoto H, Murata T, et al. Structural insights into the subtype-selective antagonist binding to the M2 muscarinic receptor. Nat Chem Biol 2018;14:1150-1158.

28. Winblad B. Piracetam: A Review of Pharmacological Properties and Clinical Uses. CNS Drug Rev 2005;11:169-182.

29. Gouhie FA, Barbosa KO, Cruz ABR, Wellichan MM, Zampolli TM. Cognitive effects of piracetam in adults with memory impairment: A systematic review and meta-analysis. Clin Neurol Neurosurg 2024;243:108358.

30. Hagan JJ, Price GW, Jeffrey P, Deeks NJ, Stean T, Piper D, Smith MI, Upton N, Medhurst AD, Middlemiss DN, et al. Characterization of SB-269970-A, a selective 5-HT(7) receptor antagonist. Br J Pharmacol 2000;130:539-548.

31. Doré AS, Okrasa K, Patel JC, Serrano-Vega M, Bennett K, Cooke RM, Errey JC, Jazayeri A, Khan S, Tehan B, et al. Structure of class C GPCR metabotropic glutamate receptor 5 transmembrane domain. Nature 2014;511:557-562.

32. MedKoo Biosciences [Internet]. Fabomotizole dihydrochloride | CAS# 189638-30-0 (2HCl) | Anxiolytic | MedKoo; [cited 2025 Mar 17]. Available from: https://www.medkoo.com/products/32719

33. Seymour PA, Schmidt AW, Schulz DW. The pharmacology of CP-154,526, a non-peptide antagonist of the CRH1 receptor: a review. CNS Drug Rev 2003;9:57-96.

34. Ivy D, Palese F, Vozella V, Fotio Y, Yalcin A, Ramirez G, Mears D, Winder DG, Cristino L, Piomelli D, et al. Cannabinoid CB2 receptors mediate the anxiolytic-like effects of monoacylglycerol lipase inhibition in a rat model of predator-induced fear. Neuropsychopharmacology 2020;45:1330-1338.

35. Li Q, Luo T, Jiang X, Wang J. Anxiolytic effects of 5-HT$_1$A receptors and anxiogenic effects of 5-HT$_2$C receptors in the amygdala of mice. Neuropharmacology 2012;62:474-484.

36. Wang S, Che T, Levit A, Shoichet BK, Wacker D, Roth BL. Structure of the D2 dopamine receptor bound to the atypical antipsychotic drug risperidone. Nature 2018;555:269-273.

37. Zheng Y, Tice CM, Singh SB. The use of spirocyclic scaffolds in drug discovery. Bioorg Med Chem Lett 2014;24:3673-3682.

38. Batista VF, Pinto DCGA, Silva AMS. Recent *in vivo* advances of spirocyclic scaffolds for drug discovery. Expert Opin Drug Discov 2022;17:603-618.

39. Basavaraja D, Doddamani SV, Athira CS, Siby A, Sreelakshmi V, Ancy A, Azeez S, Babu TS, Manjula SN, Rangappa KS, et al. Spiro-heterocycles: Recent advances in biological applications and synthetic strategies. Tetrahedron 2025;173:134468.

40. Kolomoets O, Voskoboynik O, Antypenko O, Berest G, Nosulenko I, Palchikov V, Karpenko O, Andronati S, Kovalenko S. Design, synthesis and anti-inflammatory activity of derivatives 10-R-3-aryl-6,7-dihydro-2H- [1,2,4]triazino [2,3-c]quinazolin-2-ones of spiro-fused cyclic frameworks. Acta Chim Slov 2017;64:902-910.

41. Kholodnyak SV, Schabelnyk KP, Antypenko OM, Kovalenko SI, Palchykov VA, Okovyty SI, Shishkina SV. 5,6-Dihydro- [1,2,4]triazolo [1,5-c]quinazolines. Message 4. Spirocompounds with [1,2,4]triazolo [1,5-c]quinazolines moieties. Synthesis and spectral characteristics. J Org Pharm Chem 2016;14:24-31.

42. Kholodnyak SV, Bukhtiarova NV, Shabelnyk KP, Berest GG, Belenichev IF, Kovalenko SI. Targeted search for anticonvulsant agents among spiroderivatives with 2-aryl-5,6-dihydro [1,2,4]triazolo [1,5-c]quinazoline fragment. Pharmacol Drug Toxicol 2016;1:39-47.

43. Ahmed AH, Oswald RE. Piracetam defines a new binding site for allosteric modulators of α-amino-3-hydroxy-5-methyl-4-isoxazole-propionic acid (AMPA) receptors. J Med Chem 2010;53:2197-2203.

44. Tanimukai H, Kudo T, Tanaka T, Grundke-Iqbal I, Iqbal K, Takeda M. Novel therapeutic strategies for neurodegenerative disease. Psychogeriatrics 2009;9:103-109.

45. Liu Y, Yang X, Gan J, Chen S, Xiao ZX, Cao Y. CB-Dock2: Improved Protein-Ligand Blind Docking by Integrating Cavity Detection, Docking and Homologous Template Fitting. Nucleic Acids Res 2022;50:W159-W164.

46. Jędrejko K, Catlin O, Stewart T, Anderson A, Muszyńska B, Catlin DH. Unauthorized ingredients in "nootropic" dietary supplements: A review of the history, pharmacology, prevalence, international regulations, and potential as doping agents. Drug Test Anal 2023;15:803-839.

47. Antypenko L, Shabelnyk K, Antypenko O. Anxiolytic potential of 1-methyl/4-(tert-butyl)-2'-(cycloalkyl/hetaryl)-6'H-spiro [piperidine/cycloalkane-4,5'/1,5'- [1,2,4]triazolo [1,5-c]quinazolines]. In: Proceedings of the VII International Scientific and Theoretical Conference "Scientific forum: theory and practice of research", Valencia, Spain, 31 January 2025; pp. 307-310.

48. Pylypenko OO, Sviatenko LK, Shabelnyk KP, Kovalenko SI, Okovytyy SI. Reaction of [2-(3-hetaryl-1,2,4-triazol-5-yl)phenyl]amines with ketones. DFT study. Theor Chem Acc 2024;143:35.

49. Breitmaier E. Structure Elucidation by NMR in Organic Chemistry: A Practical Guide, 3rd ed. Chichester: Wiley; 2002.

50. Antypenko L, Shabelnyk K, Antypenko O, Arisawa M, Oksenych V, Kamyshnyi O, Kovalenko S. *In silico* identification and characterization of spiro [1,2,4]triazolo [1,5-c]quinazolines as diacylglycerol kinase α modulators. Molecules 2025;30:2324.

51. Banerjee P, Kemmler E, Dunkel M, Preissner R. ProTox 3.0: a webserver for the prediction of toxicity of chemicals. Nucleic Acids Res 2024;52:W513-W520.

52. Daina A, Michielin O, Zoete V. SwissADME: a free web tool to evaluate pharmacokinetics, drug-likeness and medicinal chemistry friendliness of small molecules. Sci Rep 2017;7:42717.

53. Duman RS, Li N, Liu RJ, Duric V, Aghajanian G. Signaling pathways underlying the rapid antidepressant actions of ketamine. Neuropharmacology 2012;62:35-41.

54. Zanos P, Gould TD. Mechanisms of ketamine action as an antidepressant. Mol Psychiatry 2018;23:801-811.

55. Krystal JH, Abdallah CG, Sanacora G, Charney DS, Duman RS. Ketamine: A Paradigm Shift for Depression Research and Treatment. Neuron 2019;101:774-778.

56. Xia Z, Dudek H, Miranti CK, Greenberg ME. Calcium influx *via* the NMDA receptor induces immediate early gene transcription by a MAP kinase/ERK-dependent mechanism. J Neurosci 1996;16:5425-5436.

57. Simões AP, Silva CG, Marques JM, Pochmann D, Porciúncula LO, Ferreira S, Carvalho AR, Canas PM, Andrade GM, Fontes-Ribeiro CA, et al. Glutamate-induced and NMDA receptor-mediated neurodegeneration entails P2Y1 receptor activation. Cell Death Dis 2018;9:297.

58. Behrooz AB, Nasiri M, Adeli S, Jafarian M, Pestehei SK, Babaei JF. Pre-adolescence repeat exposure to sub-anesthetic doses of ketamine induces long-lasting behaviors and cognition impairment in male and female rat adults. IBRO Neurosci Rep 2024;16:211-223.

59. Lei X, Guo Q, Zhang J. Mechanistic Insights into Neurotoxicity Induced by Anesthetics in the Developing Brain. Int J Mol Sci 2012;13:6772-6799.

60. Zhang D, Liu J, Zhu T, Zhou C. Identifying c-fos Expression as a Strategy to Investigate the Actions of General Anesthetics on the Central Nervous System. Curr Neuropharmacol 2022;20:55-71.

61. Massara DL, Osuru HP, Oklopcic A, Milanovic D, Joksimovic SM, Caputo V, DiGruccio MR, Ori C, Wang G, Todorovic SM, et al. General Anesthesia Causes Epigenetic Histone Modulation of c-Fos and Brain-derived Neurotrophic Factor, Target Genes Important for Neuronal Development in the Immature Rat Hippocampus. Anesthesiology 2016;124:1311-1327.

62. Fidalgo AR, Cibelli M, White JP, Nagy I, Maze M, Ma D. Systemic inflammation enhances surgery-induced cognitive dysfunction in mice. Neurosci Lett 2011;498:63-66.

63. Ye Z, Li Q, Guo Q, Xiong Y, Guo D, Yang H, Yang L. Ketamine induces hippocampal apoptosis through a mechanism associated with the caspase-1 dependent pyroptosis. Neuropharmacology 2018;128:63-75.

64. Wu L, Zhang K, Sun L, Bai J, Zhang M, Zheng J. Laminin degradation by matrix metalloproteinase 9 promotes ketamine-induced neuronal apoptosis in the early developing rat retina. CNS Neurosci Ther 2020;26:1058-1068.

65. Belenichev IF, Aliyeva OG, Popazova OO, Bukhtiyarova NV. Involvement of heat shock proteins HSP70 in the mechanisms of endogenous neuroprotection: the prospect of using HSP70 modulators. Front Cell Neurosci 2023;17:1131683.

66. Farahmandfar M, Akbarabadi A, Bakhtazad A, Zarrindast MR. Recovery from ketamine-induced amnesia by blockade of GABA-A receptor in the medial prefrontal cortex of mice. Neuroscience 2017;344:48-55.

67. Davidson A, deGraaff JC. Anesthesia and Apoptosis in the Developing Brain: An Update. Curr Anesthesiol Rep 2013;3:57-63.

68. Lisek M, Mackiewicz J, Sobolczyk M, Ferenc B, Guo F, Zylinska L, Boczek T. Early Developmental PMCA2b Expression Protects From Ketamine-Induced Apoptosis and GABA Impairments in Differentiating Hippocampal Progenitor Cells. Front Cell Neurosci 2022;16:890827.

69. Shahidi S, Hashemi-Firouzi N, Afshar S, Asl SS, Komaki A. Protective Effects of 5-HT1A Receptor Inhibition and 5-HT2A Receptor Stimulation Against Streptozotocin-Induced Apoptosis in the Hippocampus. Malays J Med Sci 2019;26:40-51.

70. Pham TH, Gardier AM. Fast-acting antidepressant activity of ketamine: highlights on brain serotonin, glutamate, and GABA neurotransmission in preclinical studies. Pharmacol Ther 2019;199:58-90.

71. Frans Ö, Rimmö PA, Áberg L, Fredrikson M. Trauma exposure and post-traumatic stress disorder in the general population. Acta Psychiatr Scand 2005;111:291-299.

72. CB-Dock2. Cavity Detection Guided Blind Docking [Internet]. Available from: https://cadd.labshare.cn/cb-dock2/index.php [accessed 2025 Jan 7].

73. RCSB PDB - 5ZTY: Crystal structure of human G protein coupled receptor [Internet]. Available from: https://www.rcsb.org/structure/5ZTY [accessed 2025 Jan 9].

74. RCSB PDB - 6HUP: CryoEM structure of human full-length α1/β3/γ2L GABA(A)R in complex with diazepam (Valium), GABA and megabody Mb38 [Internet]. Available from: https://www.rcsb.org/structure/6hup [accessed 2025 Nov 7].

75. RCSB PDB - 5ZKB: Crystal structure of rationally thermostabilized M2 muscarinic acetylcholine receptor bound with AF-DX 384 [Internet]. Available from: https://www.rcsb.org/structure/5ZKB [accessed 2025 Jan 8].

76. RCSB PDB - 6CM4: Structure of the D2 Dopamine Receptor Bound to the Atypical Antipsychotic Drug Risperidone [Internet]. Available from: https://www.rcsb.org/structure/6CM4 [accessed 2025 Jan 9].

77. RCSB PDB - 8FYX: Buspirone-bound serotonin 1A (5-HT1A) receptor-Gi1 protein complex [Internet]. Available from: https://www.rcsb.org/structure/8FYX [accessed 2025 Jan 8].

78. RCSB PDB - 7XTC: Serotonin 7 (5-HT7) receptor-Gs-Nb35 complex [Internet]. Available from: https://www.rcsb.org/structure/7XTC [accessed 2025 Jan 8].

79. RCSB PDB - 3LSX: Piracetam bound to the ligand binding domain of GluA3 [Internet]. Available from: https://www.rcsb.org/structure/3LSX [accessed 2025 Jan 13].

80. RCSB PDB - 4K5Y: Crystal structure of human corticotropin-releasing factor receptor 1 (CRF1R) in complex with the antagonist CP-376395 [Internet]. Available from: https://www.rcsb.org/structure/4K5Y [accessed 2025 Jan 9].

81. RCSB PDB - 4OO9: Structure of the human class C GPCR metabotropic glutamate receptor 5 transmembrane domain in complex with the negative allosteric modulator mavoglurant [Internet]. Available from: https://www.rcsb.org/structure/4OO9 [accessed 2025 Jan 9].

82. Shabelnyk K, Fominichenko A, Antypenko O, Gaponov O, Koptieva S, Shyshkina S, Voskoboinik O, Okovytyy S, Kovalenko S, Oksenych V, Kamyshnyi O. Antistaphylococcal triazole-based molecular hybrids: design, synthesis and activity. Pharmaceuticals 2025;18:83.

83. ProTox-II - Prediction Of Toxicity Of Chemicals [Internet]. Available from: https://tox-new.charite.de/protox_II/index.php?site=home.-do [accessed 2024 May 11].

84. SwissADME [Internet]. Available from: http://www.swissadme.ch/ [accessed 2024 May 16].